Original Article

Semi-automated detection of cervical spinal cord compression with the Spinal Cord Toolbox

Magda Horáková[1,2,3]^, Tomáš Horák[1,2,3]^, Jan Valošek[4,5]^, Tomáš Rohan[2,6]^, Eva Koriťáková[7]^, Marek Dostál[2,6]^, Jan Kočica[1,2,3]^, Tomáš Skutil[1,2], Miloš Keřkovský[2,6]^, Zdeněk Kadaňka Jr[1,2]^, Petr Bednařík[3,8,9,10]^, Alena Svátková[3,11,12]^, Petr Hluštík[4,13]^, Josef Bednařík[1,2,3]^

[1]Department of Neurology, University Hospital Brno, Brno, Czech Republic; [2]Faculty of Medicine, Masaryk University, Brno, Czech Republic; [3]Central European Institute of Technology, Multimodal and Functional Imaging Laboratory, Brno, Czech Republic; [4]Department of Neurology, Faculty of Medicine and Dentistry, Palacký University Olomouc, Olomouc, Czech Republic; [5]Department of Biomedical Engineering, University Hospital Olomouc, Olomouc, Czech Republic; [6]Department of Radiology and Nuclear Medicine, University Hospital Brno, Brno, Czech Republic; [7]Institute of Biostatistics and Analyses, Faculty of Medicine, Masaryk University, Brno, Czech Republic; [8]Medical University of Vienna, Department of Biomedical Imaging and Image-guided Therapy, High Field MR Centre, Vienna, Austria; [9]Danish Research Centre for Magnetic Resonance, Centre for Functional and Diagnostic Imaging and Research, Copenhagen University Hospital Amager and Hvidovre, Hvidovre, Denmark; [10]Department of Radiology, Centre for Functional and Diagnostic Imaging and Research, Copenhagen University Hospital Amager and Hvidovre, Hvidovre, Denmark; [11]Department of Imaging Methods, Faculty of Medicine, University of Ostrava, Ostrava, Czech Republic; [12]Medical University of Vienna, Department of Medicine III, Clinical Division of Endocrinology and Metabolism, Vienna, Austria; [13]Department of Neurology, University Hospital Olomouc, Olomouc, Czech Republic

Contributions: (I) Conception and design: M Horáková, T Horák, J Valošek, J Bednařík; (II) Administrative support: P Bednařík, A Svátková, P Hluštík; (III) Provision of study materials or patients: T Horák, J Bednařík, P Bednařík, A Svátková; (IV) Collection and assembly of data: M Horáková, T Horák, J Valošek, M Keřkovský, M Dostál, T Rohan, J Kočica, T Skutil, Z Kadaňka Jr; (V) Data analysis and interpretation: M Horáková, EK, T Horák, J Valošek; (VI) Manuscript writing: All authors; (VII) Final approval of manuscript: All authors.

Correspondence to: Josef Bednařík, Department of Neurology, University Hospital Brno, Jihlavská 20, Brno, 625 00, Czech Republic.
Email: bednarik.josef@fnbrno.cz.

Background: Degenerative cervical spinal cord compression is becoming increasingly prevalent, yet the MRI criteria that define compression are vague, and vary between studies. This contribution addresses the detection of compression by means of the Spinal Cord Toolbox (SCT) and assesses the variability of the morphometric parameters extracted with it.

Methods: Prospective cross-sectional study. Two types of MRI examination, 3 and 1.5 T, were performed on 66 healthy controls and 118 participants with cervical spinal cord compression. Morphometric parameters from 3T MRI obtained by Spinal Cord Toolbox (cross-sectional area, solidity, compressive ratio, torsion) were combined in multivariate logistic regression models with the outcome (binary dependent variable) being the presence of compression determined by two radiologists. Inter-trial (between 3 and 1.5 T) and inter-rater (three expert raters and SCT) variability of morphometric parameters were assessed in a subset of 35 controls and 30 participants with compression.

Results: The logistic model combining compressive ratio, cross-sectional area, solidity, torsion and one binary indicator, whether or not the compression was set at level C6/7, demonstrated outstanding compression detection (area under curve =0.947). The single best cut-off for predicted probability calculated

^ ORCID: Magda Horáková, 0000-0003-3317-2661; Tomáš Horák, 0000-0003-1743-1133; Jan Valošek, 0000-0002-7398-4990; Tomáš Rohan, 0000-0002-7105-583X; Eva Koriťáková, 0000-0002-2268-0444; Marek Dostál, 0000-0003-1740-9227; Jan Kočica, 0000-0002-2937-6373; Miloš Keřkovský, 0000-0003-0587-9897; Zdeněk Kadaňka, 0000-0001-5146-2457; Petr Bednařík, 0000-0002-8828-7661; Alena Svátková, 0000-0002-9188-4280; Petr Hluštík, 0000-0002-1951-0671; Josef Bednařík, 0000-0001-7420-2383.

using a multiple regression equation was 0.451, with a sensitivity of 87.3% and a specificity of 90.2%. The inter-trial variability was better in Spinal Cord Toolbox (intraclass correlation coefficient was 0.858 for compressive ratio and 0.735 for cross-sectional area) compared to expert raters (mean coefficient for three expert raters was 0.722 for compressive ratio and 0.486 for cross-sectional area). The analysis of inter-rater variability demonstrated general agreement between SCT and three expert raters, as the correlations between SCT and raters were generally similar to those of the raters between one another.

Conclusions: This study demonstrates successful semi-automated compression detection based on four parameters. The inter-trial variability of parameters established through two MRI examinations was conclusively better for Spinal Cord Toolbox compared with that of three experts' manual ratings.

Keywords: Spinal cord compression (SCC); cervical spinal cord; myelopathy; magnetic resonance imaging (MRI); reproducibility

Submitted Aug 05, 2021. Accepted for publication Dec 13, 2021; Published online: 24 Jan 2022.
doi: 10.21037/qims-21-782
View this article at: https://dx.doi.org/10.21037/qims-21-782

Introduction

Degenerative cervical spinal cord compression (SCC) is becoming increasingly prevalent as global demographic change tends towards a burgeoning population of ageing people. Up to 40% of the Caucasian American/European population over the age of 60 years show MRI signs of cervical cord compression without neurological symptoms and signs (1,2), a condition termed non-myelopathic degenerative cervical cord compression (NMDC). Around 10% of patients with SCC develop neurological symptoms of compression (1), giving rise to a condition known as degenerative cervical myelopathy (DCM), which has been established as the most common cause of non-traumatic spinal cord dysfunction in adults (3).

Advanced quantitative MRI methods (such as diffusion MRI, magnetization transfer, T_2-weighted white/grey matter signal intensity ratio, and MR spectroscopy) have the capacity to detect cervical spinal cord abnormalities in NMDC patients at much the same order of differences as those that appear when DCM patients are compared with healthy controls (4-8). Several studies have identified parameters that indicate increased risk of progression to symptomatic DCM in the future, among them symptomatic cervical radiculopathy, electrophysiological abnormalities, T_2-weighted MRI hyperintensities, decreased Torg-Pavlov ratio, decreased cross-sectional area (CSA) and compressive ratio (CR) (1,4,9-12).

Although quantitative MRI techniques provide promising predictors of NMDC progression, the diagnosis of SCC is still based on conventional structural MRI. Unfortunately, the definition of SCC is vague and varies between studies, leading to bias in meta-analyses derived from global overviews, rendering multi-centre studies difficult (1). Further, repeated MRI in longitudinal follow-up of mild DCM and NMDC requires reliable quantitative measures to assess the potential progression of radiological outcomes such as CR and CSA. Personal expert evaluation is time-consuming, and investigations of its reliability are currently sparse.

In 2016, the Spinal Cord Toolbox (SCT), an open-source software package for the analysis of spinal cord MRI data was introduced (13). Among its plethora of functionalities, SCT includes tools for automated spinal cord segmentation (14) and subsequent morphometric analysis (13). SCT allows to extract routinely-used radiological measures such as right-left diameter (RL), anterior-posterior diameter (AP) and CSA but also parameters reflecting the indentation, and torsion of the spinal cord. SCT is primarily designed for quantitative analysis of the spinal cord, thus the analysis of the surrounding anatomical structures is limited.

Martin *et al.* (4) recently compared automated shape analysis of metrics computed by SCT with expert evaluation and reported excellent results. They also proposed an objective definition of SCC as deviation from normal in any of three quantitative parameters that reflect flattening, indentation, and torsion. However, the number of participants in their study was limited—20 healthy controls and 20 NMDC patients—while, for some parameters, the cut-off values were defined on the basis of only 3–7 abnormal values (flattening) or 8 abnormal values pooled

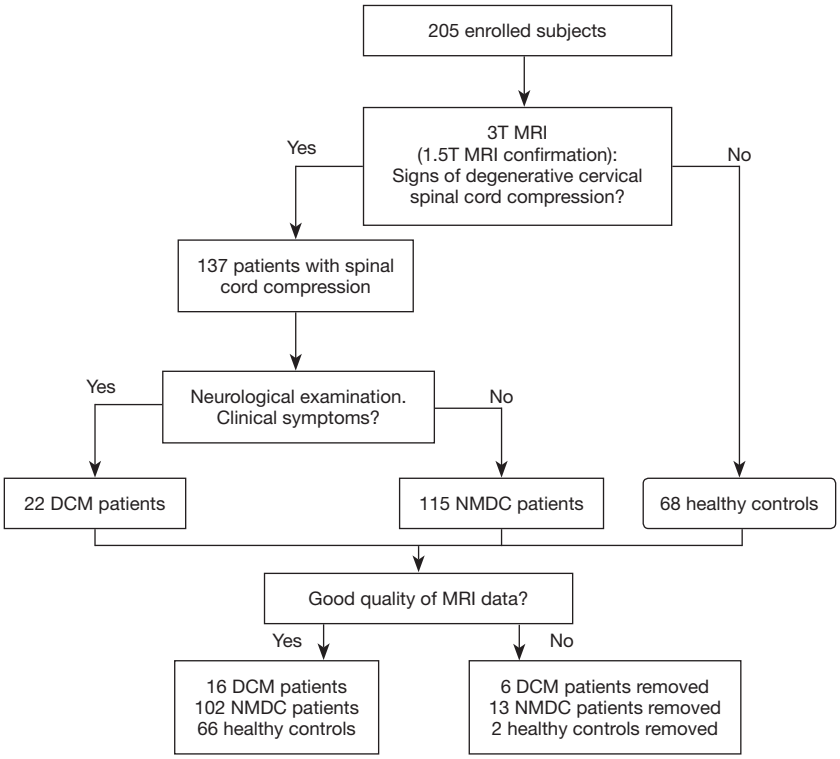

Figure 1 Flowchart of participants' recruitment. DCM, degenerative cervical myelopathy; NMDC, non-myelopathic degenerative cervical cord compression.

over different intervertebral levels (torsion).

The aim of this study is to establish a semi-automated procedure of cervical SCC detection employing the SCT-derived morphometric parameters computed from 3 T MRI data. To establish the variability of the proposed method, the methodology includes investigation of the inter-trial variability of SCT by comparing two (1.5 and 3 T) MRI scanners. A final comparison is then made between the inter-trial and inter-rater variability of experts' manual ratings and the automated assessment.

We present the following article in accordance with the STROBE reporting checklist (available at https://qims.amegroups.com/article/view/10.21037/qims-21-782/rc).

Methods

Study participants

The study was conducted in accordance with the Declaration of Helsinki (as revised in 2013). All study participants gave written informed consent, and all study procedures received approval from the institutional review board of the University Hospital Brno (No. EKV-2017-055). A total of 205 participants were enrolled, 68 of them healthy controls (HC) and 137 participants with cervical SCC, between May 2018 and May 2020. Healthy controls and SCC participants were recruited from a database of individuals at the spinal cord centre of a tertiary university hospital, all of whom had been examined in the course of parallel projects (7,8,15). SCC participants fulfilled the radiological imaging criteria for cervical cord compression. All participants with SCC were clinically examined by neurological procedures that focused on the detection of symptoms and signs of degenerative cervical myelopathy; this served to distinguish between DCM and NMDC group. The severity of disability and functional impairment was scored on the modified Japanese Orthopaedic Association (mJOA) scale. The HCs exhibited no MRI signs of cervical cord compression, were free of any known musculoskeletal disorders and had no acute medical problems. Only participants with sufficient MRI data quality were further analysed, resulting in 66 HC, 102 NMDC and 16 DCM (see *Figure 1*). MRI data from these 184 participants were submitted to semi-automated cervical spinal cord

compression detection. From this pool of participants, 35 HCs and 30 SCCs were used for a variability analysis of quantitative morphometric parameters. In this analysis, similar parameters to the SCT output were also quantified manually. Data available on request due to privacy/ethical restrictions.

MRI acquisition

Each participant had already been scanned twice, once employing 3T MRI and once employing 1.5 T MR, as part of parallel projects. For both measurements, multi-echo gradient echo (ME-GRE) sequences were used. The 3 T MRI (Prisma, Siemens, Erlangen, Germany) examination used 64-channel head/neck and 32-channel spine coils and contained axial T_2*-w, T_2-w TSE sagittal and diffusion-weighted images (15). For the purpose of this study, the axial T_2*-w MEDIC (Multi-Echo Data Image Combination) sequence covering vertebral levels C3–C7 was used (FOV 180×180 mm^2, matrix size 512×512 voxels after interpolation in Fourier domain, slice thickness 2.5 mm, 42 contiguous slices, interleaved acquisition, TR/TE =778/17 ms, 4 echoes, flip angle 30°, voxel size 0.35×0.35×2.5 mm^3 after interpolation in k-space; original voxel size 0.70×0.70×2.5 mm^3, TA =7 min 51 s).

On 1.5T MRI (Philips Ingenia, Amsterdam, The Netherlands) standard diagnostic imaging of cervical spine was performed. The protocol used 16 channel head/neck coil and included T_1-w TSE sagittal, T_2-w TSE sagittal, T_2-w TSE STIR sagittal, T_2-w TSE transversal (used for creating the report in a routine clinical practice) and the axial T_2*-w multi-echo steady-state sequence (T2 FFE—fast field echo, equivalent of MEDIC) covering C2–C7 levels with 20 contiguous slices, FOV 170×170 mm^2, acquisition matrix size 284×271 voxels, slice thickness 4.0 mm, TR/TE =478/9.2 ms, 1 echo, flip angle 25°, voxel size 0.60×0.63×4.0 mm^3, TA =4 min 37 s. The T2 FFE sequence was used for this study.

Radiological detection of cord compression, image analysis and morphometric parameters

Qualitative criteria for cervical spinal cord compression at each level were expert-rater defined as changes in spinal cord contour or shape at the level of an intervertebral disc on axial MRI scan compared with the midpoint level of neighbouring vertebrae (9,11). The reported level of spinal cord compression was confirmed on T2 TSE sagittal scan. Visual identification of spinal cord compression was performed consensually by two board-certified radiologists (MK, 18 years of practice; TR, 6 years of practice). Qualitative identification of cervical cord compression was largely made on the basis of 3 T data, and only when results were unclear were the corresponding images from the second measurement with the 1.5 T MRI scanner deployed.

Two experts manually selected the slice corresponding to each intervertebral discs C3/4, C4/5, C5/6 and C6/7 on both 1.5 T and 3T, by consensus. The C2/3 intervertebral level was not analysed. Selection of axial slices was performed in correlation with sagittal T2 TSE scans. In the case of a single acquired slice of the intervertebral space, the acquired slice was further analysed. In the case of multiple acquired slices of the intervertebral space, the slice with the lowest compression ratio was further analysed. IntelliSpace Portal Concerto v10.1 software (Philips, Best, The Netherlands) was employed for quantitative assessment of the morphometric parameters by three expert raters (Rater1 = TR, board-certified radiologist, 6 years of practice; Rater 2 = TS, medical student, 1 year of practice; Rater 3 = JK, neurologist, 5 years of practice), who measured CSA, anterior-posterior diameter (AP) and transverse diameter (RL) in these slices.

Both 3T Siemens and 1.5T Philips T2*-w axial images were processed using the SCT v4.1.0 (RRID:SCR_014170) to segment the spinal cord automatically, employing a convolution neural network algorithm (14) automatically to extract morphometric parameters for each participant utilizing the *sct_process_segmentation* function (13). All automated segmentations of the spinal cord provided by SCT were visually inspected using FSLeyes viewer (part of FSL) and spinal cord contour was manually corrected in approximately 5% HC and 30% SCC. Morphometric parameters were extracted for each individual slice, both with and without the integrated angle-correction option. The angle correction stretches the image of spinal cord within the slice on the basis of the angle between the centre-line and the axial plane. The slices corresponding to intervertebral levels were then manually selected. To be more specific, the *area* (cross-sectional area), *diameter_AP*, *diameter_RL*, *eccentricity*, *orientation* and *solidity* functions were used for further analysis.

Compression ratio was calculated as AP:RL diameter, which, together with CSA, reflected flattening of the spinal cord. Eccentricity was defined as the ratio of the focal distance over the major axis length of ellipse with the same second moments as the spinal cord, thus having similar interpretation as CR. Solidity, which was used to assess

indentation of the spinal cord, was expressed as the ratio of CSA to the area of the smallest convex polygon surrounding all positive pixels in the image (13). Torsion was calculated in three variants, based on the extracted *orientation* (∠): (I) the average of absolute differences in orientation between the slice at the intervertebral disc and one slice above and below, (II) similarly, but taking into the account two slices above and below, and (III) finally, taking into account three slices above and three slices below (see *Figure 2*):

$$torsion(v1) = \frac{1}{2}\left(\left|\angle x - \angle x_{-1}\right| + \left|\angle x - \angle x_{+1}\right|\right) \quad [1]$$

$$torsion(v2) = \frac{1}{4}\left(\left|\angle x - \angle x_{-1}\right| + \left|\angle x - \angle x_{+1}\right| + \left|\angle x_{-1} - \angle x_{-2}\right| + \left|\angle x_{+1} - \angle x_{+2}\right|\right) \quad [2]$$

$$torsion(v3) = \frac{1}{6}\left(\left|\angle x - \angle x_{-1}\right| + \left|\angle x - \angle x_{+1}\right| + \left|\angle x_{-1} - \angle x_{-2}\right| + \left|\angle x_{+1} - \angle x_{+2}\right| + \left|\angle x_{-2} - \angle x_{-3}\right| + \left|\angle x_{+2} - \angle x_{+3}\right|\right) \quad [3]$$

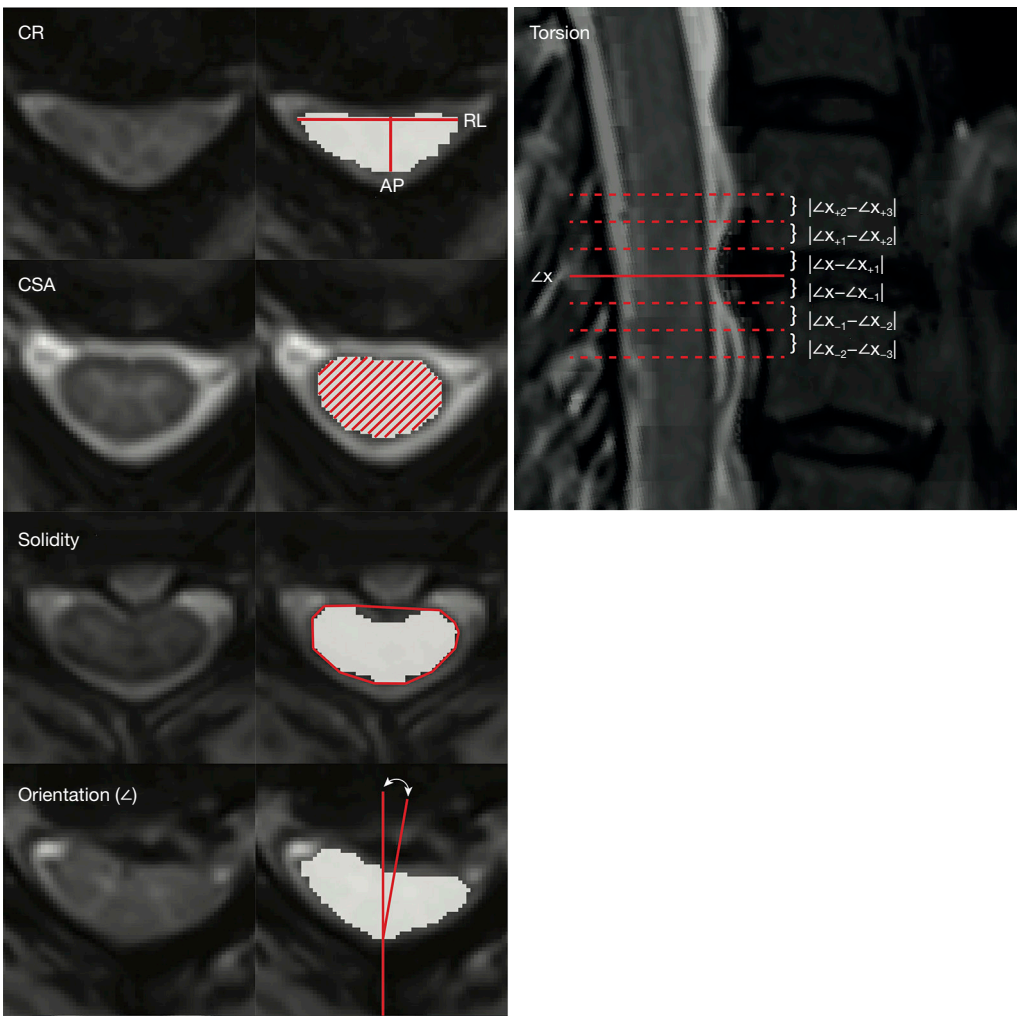

Figure 2 SCT-derived morphometric parameters. CR was calculated as AP:RL ratio. Torsion was calculated as the average of absolute differences in orientation between adjacent slices. RL, right-left diameter; AP, anterior-posterior diameter; CR, compressive ratio; CSA, cross-sectional area; SCT, Spinal Cord Toolbox.

The optimum approach was then selected on the basis of receiver operating characteristic (ROC) analysis with compression as the dependent variable. The results from two slices and three slices above and below proved to be very similar, with the latter variant considered slightly better in the light of the average area under the curve (AUC) (Table S1). Therefore, the torsion used for further analysis was calculated through the three slices with each slice thickness 2.5 mm above and below.

Neither indentation nor torsion was quantified by expert raters. No adjustments were made to defining the compression, selection of slices and experts' manual ratings in consideration of any discrepancies with semi-automated SCT analysis.

Statistical analysis

Data were analysed in SPSS version 25 (Statistical Package for the Social Sciences, IBM, Armonk, New York). All continuous variables were tested for normality by means of the Kolmogorov-Smirnov test. Continuous parameters were summarized as mean (± Standard Deviation, SD) or median (5th–95th percentile range) depending on their distribution. Categorical parameters were expressed as absolute and relative frequencies. Fisher´s exact test (for binary variables) Chí-square test for nominal variables, and the Kruskal-Wallis test and Mann-Whitney U test (for continuous variables) were employed to test differences between selected groups. Repeated measures ANOVA were employed to assess differences in morphometric parameters across the intervertebral levels and between different raters. Paired *t*-tests and Wilcoxon signed ranks sum tests were used to test differences between data with and without angle correction. Pearson/Spearman correlations were used to analyse the relationship between continuous variables, depending on their distributions. There were no missing data.

Angle correction

All morphometric parameters derived from SCT were extracted twice, once with angle correction and once without. The differences between corrected and uncorrected values were calculated and the parameters with and without correction were compared by means of paired *t*-test and Wilcoxon signed ranks test, depending on their distribution. The results of angle correction analyses appear in the Table S2. The values with angle correction were employed for the main analysis. A summary of data without angle correction appears in the Tables S3,S4.

Relationship between CR and eccentricity

Interestingly, but in agreement with the definition of eccentricity as the ratio of the focal distance over the major axis length of ellipse with the same second moments as the spinal cord, the value of the Spearman correlation between CR and eccentricity was 1 in all analyses. A scatter-plot of the relationship appears in the Appendix 1 (Figure S1). There was no significant difference between usage of CR and eccentricity throughout the study and CR was chosen only because it is easier to interpret, as well as being in more frequent use in other studies.

Normative data

The normative data of SCT-derived morphometric parameters with angle correction were expressed as mean (± SD) or median (5th–95th percentile range) depending on their distribution. ROC with AUC was plotted to assess the detection capability of morphometric parameters with angle correction in the establishment of cervical cord compression at each intervertebral level determined by the consensus of two experts. The best cut-offs were determined by Youden's index.

Semi-automated compression detection

Parameters with an AUC of >0.7 (the ability to detect compression) and a mutual correlation of less than 0.7 (due to collinearity) were used in multivariate logistic regression (for binary-coded presence of compression as an outcome) with backward stepwise removal of factors. CR was chosen as one parameter representing both AP and RL. Age and height were also included as confounding factors.

Four multivariate logistic regression model were calculated, one for each intervertebral level C3/4, C4/5, C5/6, C6/7. Further, a multivariate logistic regression pooled over all intervertebral levels was performed. The base was set to level C5/6 due to the highest number of compressions in this level and all other levels (C3/4, C4/5 and C6/7) were included in the pooled model as categorical (dummy) variables. The models were constructed over data from HC and data in levels with compression in the SCC group. Therefore, the levels without compression in SCC were not used. The approach, including levels without compressions from the SCC group as "healthy levels", appears in the Table S6. ROC analysis of the predicted probabilities of final multivariate logistic regressions was performed and three diagnostic thresholds determined: the first by maximising the Youden's index (the sum of sensitivity and specificity), the second defined

as the maximal value with sensitivity of over 90% and the third as the minimal value with specificity of over 90%. The latter two values were used to establish a borderline interval. Cross-validation of this approach was performed with random assignment of each level with compression and levels from healthy participants to six groups. Six models were then constructed, each over 5/6 of the data. ROC analysis was performed, defining the best cut-off for predicted probability employing the Youden's index. The predicted probability, and consequently sensitivity and specificity of compression detection, were then calculated in the remaining 1/6 levels.

Inter-trial and inter-rater variability of morphometric parameters

The analysis of variability took into account the RL, AP, CR and CSA from a subset of 35 HCs and 30 NMDCs, parameters obtained from both the MRI measurements employing SCT, together with the assessments from all three expert raters. The variability of solidity was also analysed, in SCT only. The differences between the two MRI measurements were calculated for SCT and each expert rater, with the equation stated as the values from 1.5 T minus the values from 3T. Intraclass correlation coefficients (ICC, two-way random, absolute agreement, single measurements) were used to compare each parameter and each rater over the two MRI measurements. Further, visualization of inter-rater and inter-trial variability was performed with multidimensional scaling. A correlation matrix (Pearson coefficients) was calculated for both CR and CSA for all raters and SCT. Then, the distances between each pair were defined as 1 minus the Pearson correlation coefficient and matrix of distances was generated. Finally, these distances were visualized in common space using two dimensions employing the multidimensional scaling.

Results

Participant characteristics

Participant characteristics appear in *Table 1*. There were 66 healthy controls and 118 participants with SCC, 102 (86.4%) of whom were asymptomatic (NMDC) and 16 (13.6%) exhibited clinical symptoms of myelopathy (DCM). The median age was 3.5 years higher in both NMDC and DCM groups. There were no statistically significant differences in sex, height, and weight. There were no significant correlations between age, weight, and any of the morphometric parameters in HC, although there was a significant correlation between height and RL diameter ($0.436<r<0.513$), CR ($-0.183<r<0.336$) and CSA ($0.340<r<0.445$) at each level. Similarly, in the variability subset, the median age was higher in the NMDC group, although significance could not be established due to the low number of participants. Age and height were therefore considered confounding factors in multivariate analysis. The median interval between the two MRI examinations was 11 days and there was no significant difference between the groups.

Normative data and proposed thresholds

Table 2 summarizes the SCT-derived morphometric parameters of HC (normative data) and of SCC participants with compression at given intervertebral levels. All individual parameters showed moderate capacity to detect compressions based on ROC analysis of each metric in relation to the presence of compression. However, the cut-offs were close to one standard deviation (SD) from the mean and within the 5th–95th percentile for solidity and torsion. Both sensitivity and specificity exceeded 80% for only a few parameters. Repeated measures ANOVA with Bonferroni corrections in HC showed significant differences ($P_{corr}<0.003$) between intervertebral levels in CR (except for C4/5 compared with C6/7) and CSA (except levels C4/5 and C5/6 compared with C6/7). In contrast, only a borderline significant difference emerged between solidity at C3/4 compared with other levels ($0.030<P_{corr}<0.043$); otherwise, solidity did not differ between levels. Finally, there was no difference in torsion between levels C3/4, C4/5 and C5/6, but all of them differed from level C6/7 ($P_{corr}<0.002$).

Compression detection

The variables included in the multivariate logistic model were age, height, CR, CSA, solidity, and torsion for each intervertebral level. The pooled model included CR, CSA, solidity, torsion, and intervertebral level (expressed as dummy variables with the base set at level C5/6). At each level (except C3/4) four factors remained significant: CR, CSA, solidity, and torsion. At level C3/4, only CR and CSA remained significant; this, however, was attributed to the low number of compressions at this level and used the same four factors to retain consistency of results. For the pooled model, CR, CSA, solidity, torsion, together with whether or not compression set at level C6/7 remained significant. The

Table 1 Characteristics of all participants and the subset of participants used for reliability analysis

Characteristics	HC, n=66	NMDC, n=102	DCM, n=16	P value
All participants				
Age (years)	53.5 (41.0, 70.7)	57.0 (42.2, 72.9)	57.0 (35.0, 76.8)	0.042*
Sex	Female: 42 (63.6%); male: 24 (36.4%)	Female: 57 (55.9%)	Female: 9 (56.3%)	0.595
Height (cm)	170 (156, 186)	170 (156, 186)	170 (147, 181)	0.422
Weight (kg)	80 (51, 105)	79 (55, 110)	79 (62, 102)	0.996
Number of patients with compression at level				
C3/4		19	5	
C4/5		55	10	
C5/6		76	13	
C6/7		39	3	
mJOA score		18 (18, 18)	15 (9, 17)	
Variability subset	HC, n=35	NMDC, n=30		
Age (years)	51.3 (40.5, 71.5)	58.8 (41.6, 72.2)		0.060
Sex	Female: 21 (60.0%); male: 14 (40.0%)	Female: 16 (53.3%); male: 14 (46.7%)		0.623
Height (cm)	174 (158, 193)	171 (157, 183)		0.282
Weight (kg)	80 (52, 100)	78 (61, 113)		0.828
Interval between MRIs (days)	10.0 (2.0, 75.0)	13.5 (1.0, 84.2)		0.683
Number of patients with compression at level				
C3/4		4		
C4/5		14		
C5/6		22		
C6/7		15		

Expressed as count, median (5th–95th percentile) or percentage. Kruskal-Wallis test used for continuous variables for comparison of all participants, Mann-Whitney test for reliability subset. Chí-square test was used for nominal variables for all participants, Fisher's exact test for reliability subset. HC, healthy controls; NMDC, non-myelopathic degenerative cervical cord compression; DCM, degenerative cervical myelopathy.

results are summarized in *Table 3*.

The parameters of each model were very similar, and the pooled model demonstrated outstanding compression discrimination (AUC = 0.947). The latter model explained 73.6% of data variability (Nagelkerke R^2 =0.736). The probability for each participant can be calculated by means of:

$$p = \frac{e^{(57.501-0.273*CR-0.102*CSA-0.408*solidity+2.168*torsion-2.729*C6/7)}}{1+e^{(57.501-0.273*CR-0.102*CSA-0.408*solidity+2.168*torsion-2.729*C6/7)}} \quad [4]$$

The thresholds for compression detection were defined by ROC analysis. The borderline interval of predicted probabilities (with the boundaries defined as a maximum value of sensitivity of over 90% and the minimum value with a specificity of over 90%) was 0.345–0.451. All cut-offs of predicted probability under 0.345 exhibited a sensitivity of 90% or more, and all cut-offs above 0.451 exhibited a specificity of 90% or more. The best single cut-off was determined by Youden index at 0.451, with sensitivity 87.3%, specificity 90.2%, positive predictive value

Table 2 Normative data and data from levels with compression for parameters extracted with SCT with angle correction

	Healthy controls	Levels with compressions	Cut-off	AUC (95% CI)	Sensitivity (%)	Specificity (%)
RL (mm)						
C3/4	12.6±1.1	13.1±1.2				
C4/5	13.3±1.1	13.7±1.2				
C5/6	13.2±1.1	13.3±1.5				
C6/7	12.1±1.2	12.3±1.1				
AP (mm)						
C3/4	7.3±0.5	6.0±0.8				
C4/5	7.3±0.6	6.2±0.8				
C5/6	7.0±0.6	6.1±0.7				
C6/7	6.6±0.6	5.7±0.6				
CR (%)						
C3/4	58.7±6.3	46.0±6.2	52.0	0.943 (0.894, 0.992)	87.5	90.9
C4/5	55.1±6.4	45.7±6.8	51.1	0.854 (0.791, 0.918)	83.1	75.8
C5/6	53.4±6.2	46.1±6.5	49.6	0.792 (0.723, 0.862)	68.5	77.3
C6/7	54.8±6.1	46.7±5.6	50.2	0.844 (0.768, 0.92)	78.6	81.8
CSA (mm^2)						
C3/4	71.7±8.2	59.5±11.1	65.7	0.874 (0.782, 0.966)	87.5	81.8
C4/5	75.4±8.6	64.4±10.1	68.4	0.807 (0.732, 0.882)	70.8	81.8
C5/6	71.4±9.3	60.7±10.8	61.0	0.781 (0.71, 0.853)	56.2	90.9
C6/7	62.3±8.9	53.4±8.2	56.7	0.778 (0.687, 0.87)	71.4	78.8
Solidity (%)						
C3/4	96.8 (95.1–98.3)	94.4 (88.4–98.0)	95.5	0.857 (0.753, 0.961)	70.8	95.5
C4/5	96.4 (94.1–97.8)	94.8 (87.8–97.8)	95.9	0.744 (0.658, 0.83)	72.3	71.2
C5/6	96.3 (94.0–98.0)	94.6 (85.8–97.2)	94.7	0.773 (0.701, 0.845)	55.1	90.9
C6/7	96.4 (93.8–98.3)	94.7 (91.1–97.5)	95.1	0.754 (0.658, 0.849)	64.3	77.3
Torsion (degree)						
C3/4	0.81 (0.45–2.01)	1.48 (0.49–3.61)	1.23	0.737 (0.607, 0.868)	62.5	86.4
C4/5	0.75 (0.25–1.61)	1.25 (0.49–2.87)	0.78	0.764 (0.683, 0.844)	83.1	60.6
C5/6	0.88 (0.44–1.65)	1.37 (0.61–3.18)	1.09	0.774 (0.701, 0.847)	75.3	71.2
C6/7	1.18 (0.53–2.76)	2.10 (0.52–3.84)	2.03	0.719 (0.615, 0.824)	54.8	87.9

Data are presented as mean ± SD where normally distributed, median (5th–95th percentile) for data without normal distribution. The values are calculated from 66 HC: 24 compressions at C3/4 level, 65 at C4/5 level, 89 at C5/6 level and 42 at C6/7 level. ROC analysis served to compare the quantitative parameters with expert qualitative assessment of the presence of compression. For data without angle correction, see Table S3. AUC, area under curve; CI, confidence interval; RL, right-left diameter; AP, anterior-posterior diameter; CR, compressive ratio; CSA, cross-sectional area; SCT, Spinal Cord Toolbox.

Table 3 Models for semi-automated compression detection employing morphometric parameters with angle correction (for data without angle correction see Table S4)

	Coefficients	OR (95% CI)	P value (factors)	P value (model)	Nagelkerke R^2	AUC (95% CI) of predicted probabilities
C3/4				<0.0005	0.843	0.979 (0.952, 1.000)
Constant	58.300		0.061			
CR (%)	−0.530	0.588 (0.413, 0.838)	0.005			
CSA (mm^2)	−0.167	0.846 (0.721, 0.992)	0.038			
Solidity (%)	−0.233	0.792 (0.392, 1.598)	0.308			
Torsion (degree)	2.369	10.690 (0.434, 263.133)	0.188			
C4/5				<0.0005	0.725	0.943 (0.904, 0.982)
Constant	54.361		0.003			
CR (%)	−0.268	0.765 (0.673, 0.869)	<0.0005			
CSA (mm^2)	−0.108	0.898 (0.831, 0.970)	0.006			
Solidity (%)	−0.375	0.687 (0.476, 0.992)	0.045			
Torsion (degree)	2.629	13.853 (3.534, 54.303)	<0.0005			
C5/6				<0.0005	0.706	0.939 (0.903, 0.975)
Constant	67.088		0.002			
CR (%)	−0.191	0.826 (0.739, 0.923)	0.001			
CSA (mm^2)	−0.069	0.933 (0.880, 0.989)	0.020			
Solidity (%)	−0.593	0.553 (0.356, 0.857)	0.008			
Torsion (degree)	3.506	33.314 (7.500, 147.973)	<0.0005			
C6/7				<0.0005	0.800	0.964 (0.930, 0.997)
Constant	90.540		0.002			
CR (%)	−0.464	0.629 (0.509, 0.777)	<0.0005			
CSA (mm^2)	−0.199	0.819 (0.734, 0.915)	<0.0005			
Solidity (%)	−0.620	0.538 (0.310, 0.934)	0.028			
Torsion (degree)	1.989	7.311 (2.349, 22.752)	0.001			
Pooled model				<0.0005	0.736	0.947 (0.928, 0.966)
Constant	57.501		<0.0005			
CR (%)	−0.273	0.761 (0.712, 0.813)	<0.0005			
CSA (mm^2)	−0.102	0.903 (0.868, 0.939)	<0.0005			
Solidity (%)	−0.408	0.665 (0.535, 0.826)	<0.0005			
Torsion (degree)	2.168	8.744 (4.809, 15.900)	<0.0005			
Level C6/7 (yes or no)	−2.729	0.065 (0.026, 0.162)	<0.0005			

Models were constructed over data from HC and from levels with compression in SCC. OR, odds ratio; CI, confidence interval; AUC, area under curve.

88.1% and negative predictive value 89.5%. The cross-validation of this approach appears in Table S5. The overall sensitivity of compression detection in validation data (i.e., participants that were not used for model construction) was 0.836, specificity 0.905, positive predictive value 0.880 and negative predictive value 0.869.

The minimum predicted probability of any compression in the DCM group was 0.484, each DCM patient had at least one compression at a probability of over 0.764, and the median of maximal probabilities in the DCM group was 0.985.

The approach including levels without compressions from the SCC group as "healthy levels" appears in the Table S6. The AUC for predicted probability in the pooled model using this approach was 0.906.

The odds ratios (ORs) for CR, CSA and solidity were consistently below 1 for all models, while the OR of torsion was significantly higher than 1. Depending on the exact model, a drop of 1% in CR increases the risk of compression by 1.2–1.7×, a drop in CSA of 10 mm^2 increases risk of compression 2.0–7.3×, a drop in solidity of 1% increases the risk of compression 1.3–1.9× and an increase in torsion of one degree increases the risk of compression 7.3–33.3 times. The categorical predictor, compression situated at level C6/7, significantly decreases the risk compared with other levels, which accords with the fact that the normal values of CSA and torsion at level C6/7 would be abnormal at other levels. *Figure 3* shows examples of morphometric parameters and the resulting predicted probability of compression in healthy control and participants with various severity of compressions.

Analysis of DCM compared to NMDC group

There were 16 (13.6%) DCM patients in the SCC group. The percentage of DCM in the SCC group bore an approximate resemblance to the estimated prevalence of DCM (1). The comparison of morphometric parameters and predicted probabilities calculated from the pooled model between the compression in NMDC and DCM group is shown in Table S7. There was no significant difference between these two groups, except for CSA at levels C3/4 (62.7 *vs.* 47.1 mm^2) and C4/5 (65.5 *vs.* 58.0 mm^2), however, this significance did not pass the correction for multiple testing and the number of subjects with compression was very low in both groups. The ROC analysis of all parameters and predicted probability did not find any well performing discriminating parameter to distinguish between NMDC and DCM. The only AUC > 0.7 were for CSA in C3/4 and C4/5 already mentioned and for solidity and predicted probability in C3/4. None of the compressions in DCM were undetected and the median of maximal predicted probabilities in DCM patients was 0.985.

Inter-trial and inter-rater variability of morphometric parameters

The differences in morphometric parameters for each expert rater and SCT with and without angle correction between the two MRI examinations appear in *Table 4* and *Figure 4*. Based on these results, SCT performed better than any of the three expert raters. The differences between SCT values with angle correction were generally slightly smaller, and ICC slightly better. The relevant table, divided into HC and SCC, appears in the Table S8.

Comparison of the inter-trial variability relative to inter-rater variability using multidimensional scaling is shown in *Figure 5*. It should be viewed as a map of distances; the higher the distance between each pair, the lower the Pearson correlation coefficient between the pair. *Figure 5* provides an approximate illustration of the agreement of SCT with expert raters since the former lay in quite close proximity to the cluster of expert raters. It also demonstrated that, in general, the values from each measurement correlated more closely in SCT compared with expert raters. Further, it shows very close correlation between SCT values with and without angle correction. The complete correlation matrices are shown in Table S9.

Discussion

Summary of findings

This study introduced semi-automated detection of compression in the cervical spinal cord, employing an open-source SCT software package. It demonstrated lower inter-trial variability of quantitative morphometric parameters extracted with SCT than that established by expert manual ratings. This approach, therefore, could well prove ideal for consistency across longitudinal and multi-centre studies, something that is acutely lacking in current research. The results indicated outstanding compression discrimination, combining four radiological parameters extracted with SCT from conventional MRI (CR, CSA, solidity, torsion) and one binary indicator of being the level C6/7 or not, into the logistic model.

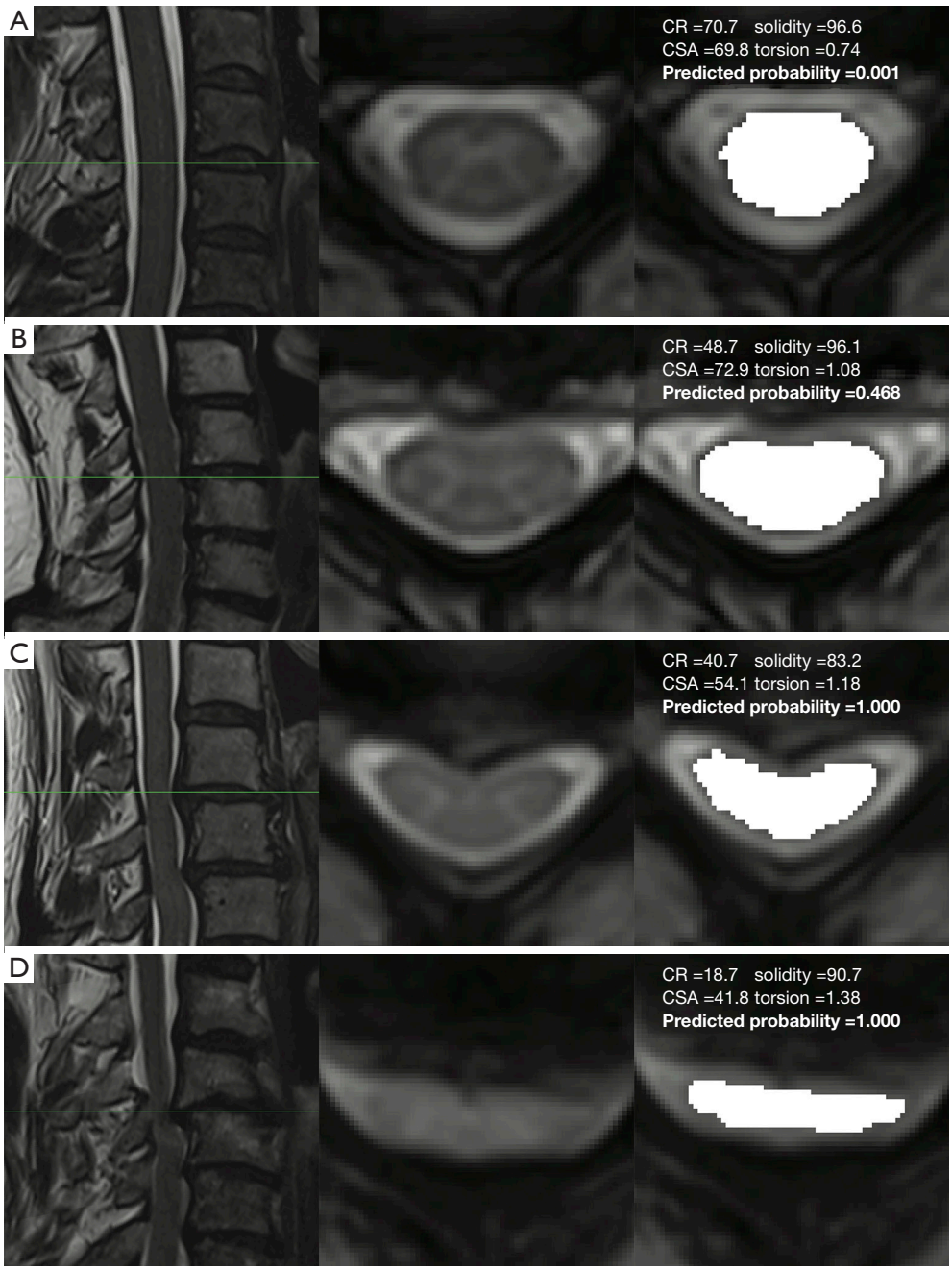

Figure 3 Examples of relation between morphometric parameters and predicted probability of compression in healthy control and various compressions. (A) Healthy control with normal parameters and low predicted probability of compression, (B) NMDC participant, (C) DCM participant with extremely low solidity, (D) DCM participant with extremely low CR. NMDC, non-myelopathic degenerative cervical cord compression; DCM, degenerative cervical myelopathy; CR, compressive ratio.

Table 4 Differences in morphometric parameters between the two MRI examinations (3 and 1.5 T) in 35 HCs and 30 SCCs

	SCT (without angle correction)	SCT (with angle correction)	Rater 1	Rater 2	Rater 3
RL (mm)					
C3/4	0.52 (–0.34, 1.18)	0.50 (–0.35, 1.17)	1.00 (0.30, 1.70)	0.34 (–0.64, 1.09)	0.76 (0.02, 1.56)
C4/5	0.61 (–0.38, 1.43)	0.60 (–0.37, 1.46)	1.00 (0.43, 1.57)	0.32 (–0.64, 1.27)	0.68 (–0.42, 2.99)
C5/6	0.45 (–0.37, 1.46)	0.42 (–0.37, 1.46)	0.80 (–0.37, 1.70)	0.17 (–0.66, 1.1)	0.62 (–1.03, 2.11)
C6/7	0.5 (–0.23, 1.34)	0.48 (–0.22, 1.33)	0.8 (–0.2, 1.6)	0.2 (–0.79, 1.16)	0.54 (–1.25, 2)
ICC	0.832 (0.289, 0.935)	0.832 (0.290, 0.935)	0.678 (–0.055, 0.883)	0.815 (0.751, 0.862)	0.631 (0.264, 0.795)
AP (mm)					
C3/4	0.58 (–0.4, 1.17)	0.57 (–0.38, 1.19)	1.40 (0.63, 2.14)	0.53 (–0.55, 1.34)	0.75 (–0.28, 1.84)
C4/5	0.25 (–0.23, 1.01)	0.27 (–0.23, 1)	1.20 (0.46, 1.9)	0.60 (–0.36, 1.30)	0.92 (–0.70, 2.10)
C5/6	0.37 (–0.29, 0.99)	0.33 (–0.29, 0.97)	1.10 (0.43, 1.97)	0.41 (–0.54, 1.27)	0.73 (–0.45, 1.74)
C6/7	0.46 (–0.17, 1.44)	0.37 (–0.18, 1.14)	1 (0.33, 2.27)	0.4 (–0.63, 1.3)	0.64 (–0.72, 2.44)
ICC	0.722 (0.169, 0.879)	0.731 (0.191, 0.882)	0.356 (–0.067, 0.706)	0.677 (0.311, 0.826)	0.459 (0.014, 0.698)
CR (%)					
C3/4	2.09 (–4.22, 7.10)	2.22 (–3.83, 7.15)	6.46 (0.65, 11.48)	1.82 (–5.5, 9.06)	2.46 (–3.71, 10.00)
C4/5	0.67 (–5.45, 4.25)	0.66 (–5.76, 4.20)	6.14 (0.51, 10.85)	2.91 (–2.75, 7.23)	3.55 (–5.15, 10.95)
C5/6	0.66 (–4.75, 7.2)	0.66 (–4.82, 7.25)	5.56 (1.37, 11.03)	2.69 (–4.09, 9.4)	2.73 (–8.01, 12.77)
C6/7	0.87 (–3.85, 10.13)	0.83 (–4.05, 8.21)	6.86 (–1.95, 13.77)	2.32 (–4.35, 9.11)	2.59 (–6.9, 14.44)
ICC	0.851 (0.801, 0.888)	0.858 (0.814, 0.891)	0.647 (–0.079, 0.876)	0.817 (0.627, 0.898)	0.703 (0.527, 0.804)
CSA (mm^2)					
C3/4	8.5 (–4.8, 15.4)	8.3 (–4.8, 15.4)	15.0 (8.0, 24.7)	4.0 (–4.7, 14.0)	10.0 (–3.4, 21.0)
C4/5	6.4 (–2.3, 15.3)	6.5 (–2.5, 15.3)	13.0 (4.3, 24.0)	5.0 (–5.0, 13.7)	11.0 (–12.7, 31.8)
C5/6	6.8 (–4.7, 13.7)	6.3 (–4.6, 13.6)	12.0 (–1.7, 22.1)	2.0 (–15.7, 13.7)	10.0 (–10.5, 25.1)
C6/7	7.3 (–0.9, 14.9)	6.7 (–0.6, 14.1)	12.0 (0.3, 26.4)	3.0 (–11.4, 14)	10.0 (–13.0, 34.8)
ICC	0.725 (0.021, 0.896)	0.735 (0.042, 0.900)	0.367 (–0.088, 0.702)	0.717 (0.610, 0.792)	0.373 (–0.018, 0.620)
Solidity (%)					
C3/4	–0.54 (–3.79, 2.53)	–0.63 (–3.75, 1.91)			
C4/5	–0.36 (–4.15, 1.40)	–0.55 (–4.07, 1.65)			
C5/6	–0.75 (–4.25, 2.24)	–0.84 (–4.04, 2.16)			
C6/7	–0.76 (–4.42, 3.21)	–0.88 (–4.23, 2.81)			
ICC	0.536 (0.412, 0.635)	0.552 (0.406, 0.660)			

The equation was stated as the values from 1.5 T minus the values from 3T. Data are summarized as median (5th–95th percentile). ICCs (two-way random, absolute agreement, single measures) with 95% CI compare each parameter pooled per all intervertebral levels between the two examinations (P<0.0005 in each parameter and rater). ICC, intra-class correlation coefficient; SCT, Spinal Cord Toolbox; RL, right-left diameter; AP, anterior-posterior diameter; CR, compressive ratio; CSA, cross-sectional area.

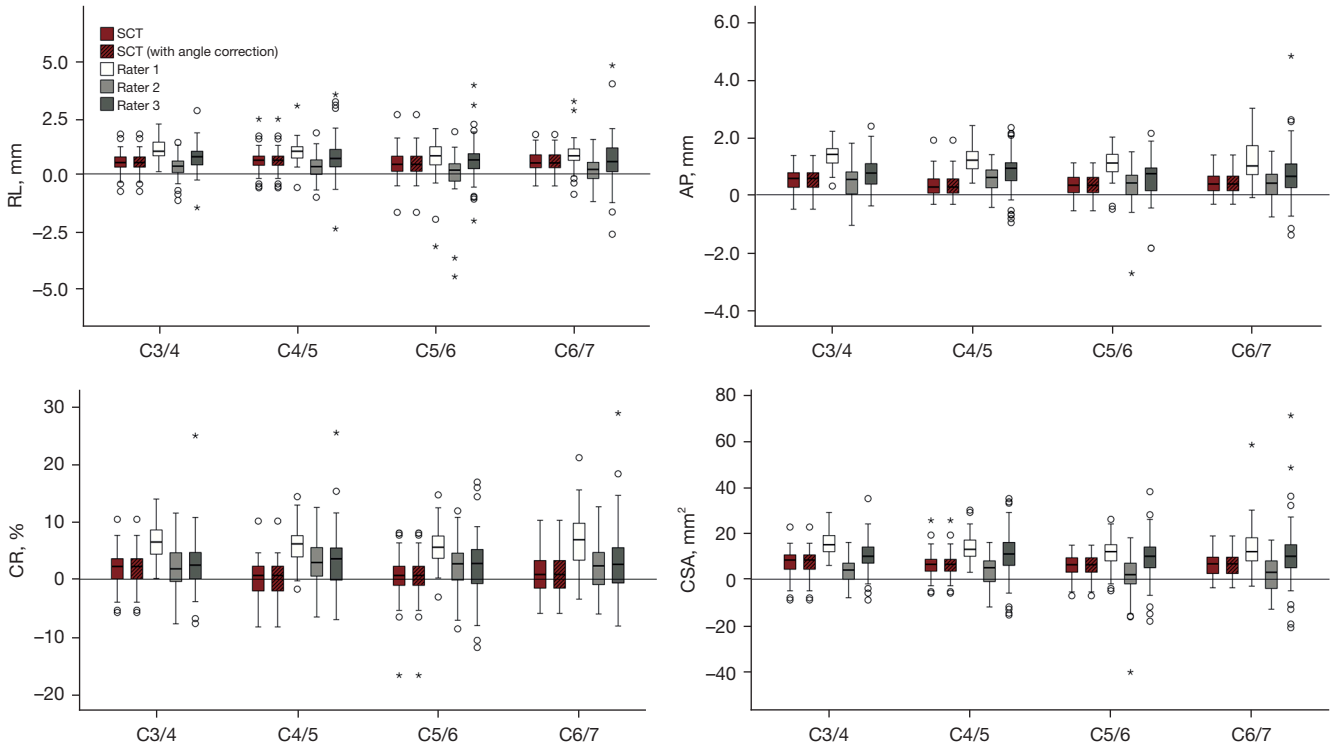

Figure 4 Differences in morphometric parameters between the two MRI examinations (3 and 1.5 T). Data pooled for HC and SCC. The bars represent 25th–75th percentiles, whiskers denote the lowest and the highest values, excluding mild outliers, which appear as dots (values greater than 1.5 times the interquartile range) and extreme outliers that appear as asterisks (values greater than 3 times the interquartile range). Medians appear as horizontal lines within the bars. RL, right-left diameter; AP, anterior-posterior diameter; CR, compressive ratio; CSA, cross-sectional area.

Further, the variability between the two MRI examinations was conclusively smaller in SCT compared with the three expert raters. The ICCs showed excellent inter-trial variability of CR (0.858) and good in CSA (0.735). There were surprising discrepancies in variability between the raters; one was very close to the standard of SCT, while the other two made systematic errors of either overestimation of the measures in 1.5T MRI or underestimation of the measures in 3T MRI.

The degree of agreement between the results extracted with SCT and the results of expert raters also became evident, as the correlations between SCT and expert raters were generally similar to those of the raters between one another.

Previous studies

To the best of our knowledge, only a few similar studies have been performed (4,16,17). Martin *et al.* (4), covered a much lower number of participants (20 HC and 20 NMDC, compared to the 66 HC and 102 NMDC and 16 DCM herein). They also addressed compression detection in a different way, as they defined compression as deviation from normal in flattening, indentation and/or torsion, and the ROC analysis was performed over these parameters separately. In contrast, our study did not assess flattening, indentation, and torsion manually, deploying only one binary indicator—the presence of compression. Thus, the data herein does not show the discriminating powers of individual parameters separately. All four parameters (CR, CSA, solidity, and torsion) in our data showed good ability to detect compression with AUCs around 0.8. However, the cut-offs were close to one SD from normal. Therefore, we combined the four parameters in a multivariate logistic model receiving excellent results. Further, the data herein did not replicate the Martin *et al.* finding that rostral CSA was significantly higher in SCC; our results indicate a C3/4 CSA mean of 72.6 mm^2 in HC, 67.4 mm^2 in NMDC and

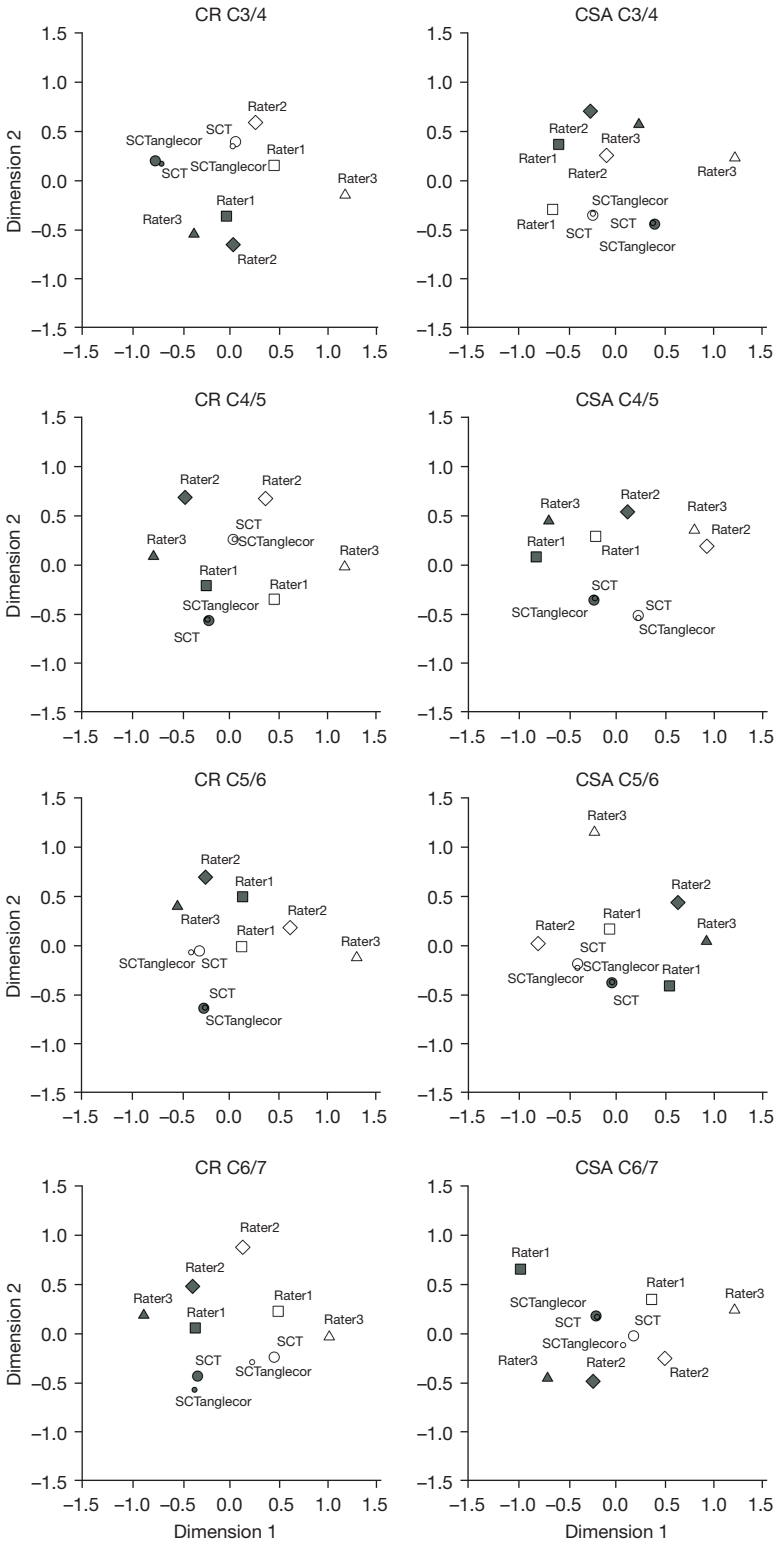

Figure 5 Inter-trial variability and inter-rater variability of morphometric parameters. The distance is defined as 1 minus r (Pearson correlation coefficient) in two-dimensional space. Empty symbols signify 1.5 T MRI measurements, filled symbols signify 3 T. CR, compressive ratio; CSA, cross-sectional area.

55.8 mm^2 in DCM. The findings herein accord with reports of spinal cord atrophy above the level of compression (18-20). Papinutto (16) investigated the reliability of CSA in 12 healthy volunteers in three different 3T MR scanners and the ICCs were in range of 0.79–0.95. Ost *et al.* (17) demonstrated that most of the SCT derived metrics lack the sufficient differentiation across mJOA score severity in DCM; however, the means of CSA, solidity and eccentricity extracted from the entire spinal cord volume were significantly related to mJOA.

Other minor findings

The normative data herein corresponded with the physiological anatomy of the spinal cord, including increases in CSA at levels C4/5 and C5/6 due to cervical enlargement and an increase in torsion at level C6/7 arising out of cervical lordosis. The substantial decline in CSA and increase in torsion at level C6/7 is probably strong justification for the inclusion of the binary C6/7 factor in the pooled logistic model.

We did not find any well performing discriminating parameter to distinguish NMDC and DCM participants. Neither the predicted probability calculated from the pooled model showed any significant differences in DCM compared to NMDC group, even though none of the compressions in DCM were undetected.

The *angle-corr* function available in SCT is a useful tool, lending further slight improvements to the inter-trial variability of SCT-derived morphometric parameters between the two MRI examinations, but the differences between corrected and uncorrected values are very small compared with those of inter-rater or inter-trial variability.

The estimates for RL, AP and CSA were generally larger in 1.5 T scanner compared to 3T scanner. The exact reason for this effect is unknown but might be attributed to the higher in-place resolution of the 3 T MEDIC sequence and usage of 4 echoes compared to 1 echo in 1.5 T FFE sequence, resulting in smaller partial volume effect between SC and CSF and better contrast for 3 T sequence, paradoxically leading to "smaller" values. The systematic error in different manufacturers and different protocols has already been published previously (21).

Limitations

The main limitation of this study is the general lack of a gold standard for compression detection that might have otherwise served for comparison with its results. This study is therefore based on qualitative determination of compression presence reflected in changes in spinal cord contour or shape. We tried to overcome this limitation by using the consensus ratings of two experienced radiologists and further, two MRI measurements from two different MRI scanners were available in the event of doubt.

Second, the approach herein is not fully automated, as the slices corresponding to intervertebral levels were chosen in person rather than by automated labelling of vertebrae. We opted for this approach after discovering the need for manual correction of the automated labelling in 20% of the first sample. Nevertheless, this limitation could be overcome in future developments in SCT that may feature an improved version of the algorithm for spinal cord labelling. It may even be possible that there exists no necessity for precise selection of intervertebral level, as the software could mark all slices with possible compressions and the expert rater would then check only these slices.

Since SCT is a tool primary designed for quantitative analysis of the spinal cord, assessment of the surrounding structures (such as vertebrae, intervertebral discs, cerebrospinal fluid) is limited. This is a limitation compared to expert raters, who might include the surrounding anatomy in their decision. However, even though the only input of the compression detection via SCT was the shape of segmented spinal cord (and manually chosen slices corresponding to intervertebral levels), the agreement between SCT and experts was excellent. Further, since both 1.5 and 3 T protocols were primarily designed for other projects (7,15), we did not acquire isotropic 3D T1w and T2w image that would be also suitable for SC segmentation.

The inter-trial variability analyses were performed over two different MRI scanners with two different protocols: on 3 T with 42 slices and 1.5 T with 20 slices. The correlation coefficients could further improve if two matching MRI scanners were employed with the same protocols. The different scanners also limited torsion calculation in 1.5 T MR; the slices were too thick (4 mm) in this protocol; at the same time, similar variants of torsion calculation to those used in 3T did not demonstrate the ability to discriminate between HC and compression (AUC within a range of 0.415–0.586). Performance of the same compression detection via 1.5 T data therefore proved impossible. Nevertheless, this approach better represents the reality of multicentre studies, and this study showed that SCT is

more reliable than expert raters, even in this situation. The ICC of solidity in the data herein was also low (0.636 in SCC group but minus 0.040 in the HC group), but it could also arise out of the low variability of solidity values in the healthy controls.

As already pointed out in the Results section, levels without compression in the SCC group were not used in the model construction shown in main text. The reason for this was possible atrophy and changes in the spinal cord even above or below the level of compression. However, an alternative approach, including levels without compressions as "healthy", appears in the Table S6 and the results remain very promising (with AUC of the pooled model at 0.906).

The number of DCM in our study was very small and the vast majority of DCM participants had compressions at multiple levels and there was no way to determine which one had been responsible for clinical myelopathy. We could not, therefore, investigate separately the parameters of compressions causing neurological symptoms. We also did not investigate the difference in Torg-Pavlov ratios between these groups.

We did not include the intervertebral level C2/3 in the analysis due to the fact, that the 3T sequence covered vertebral levels C3–C7, as it was primarily designed for other parallel projects (8,15), however, there was only one participant with compression in level C2/3 based on the 1.5 T MRI examination covering C2–C7.

Only one of the three expert raters manually measuring RL, AP and CR was board-certified radiologist. However, all raters completed training of spinal cord measurement. Further, based on the result of inter-trial variability, Rater 2 (TS, medical student) had the highest values of ICCs.

Conclusions

This study demonstrated successful semi-automated detection of cervical spinal cord compression based on four SCT-derived morphometric parameters. The parameters extracted using SCT exhibited lower variability than the experts' manual ratings in RL, AP, CR and CSA. Further, SCT enabled exact quantification of indentation and torsion. Introduction of SCT into radiological evaluations may bring more reliable results to longitudinal and multi-centre studies. The approach also saves a great deal of time, perhaps enabling its routine use in the assessment of the natural course of NMDC and mild DCM; the rate of progression may well become a valid predictor of whether the patient would benefit from surgery or not.

Acknowledgments

Data were partially presented at CSRS 49th Annual Meeting, Atlanta, December 1-4th 2021 as e-poster. We thank Dr. Julien Cohen-Adad (University of Montreal, Canada) for comments on the manuscript. We thank Tony Long (Carsphairn, Scotland), who helped work up the English and Dagmar Kratochvílová (University Hospital Brno, Czech Republic) for participants recruitment. We thank the core facility of the Multimodal and Functional Imaging Laboratory, Masaryk University, CEITEC, supported by MEYS CR (LM2018129 Czech-BioImaging) and all those who facilitated access to computing and storage facilities owned by parties and projects contributing to the MetaCentrum National Grid Infrastructure provided under the program "Projects of Large Research, Development, and Innovations Infrastructures" (CESNET LM2015042).

Funding: This research was funded by a Czech Health Research Council grant (ref. NV18-04-00159), and by the Ministry of Health of the Czech Republic project for conceptual development in research organizations, (ref. 65269705, University Hospital, Brno, Czech Republic and ref. 00098892, University Hospital Olomouc), and project of specific research (ref. MUNI/A/1600/2020) from the program of support for student projects at Masaryk University, Brno. AS received funding from the European Union Horizon 2020 research and innovation program under Marie Skłodowska-Curie grant agreement (No. 794986). PB was supported by the European Union Horizon 2020 research and innovation program under Marie Skłodowska-Curie grant agreement (No. 846793), and by a NARSAD Young Investigator Grant from the Brain and Behavior Research Foundation (No. 27238).

Footnote

Reporting Checklist: The authors have completed the STROBE reporting checklist. Available at https://qims.amegroups.com/article/view/10.21037/qims-21-782/rc

Conflicts of Interest: All authors have completed the ICMJE uniform disclosure form (available at https://qims.amegroups.com/article/view/10.21037/qims-21-782/coif). MH, TH, JK, TS, ZK, PB, AS and JB report that this research was supported by Czech Health Research Council grant (ref. NV18-04-00159), Ministry of Health of the Czech Republic (ref. 65269705) and The Ministry

of Education, Youth and Sports of the Czech Republic (ref. MUNI/A/1600/2020). JV and PH report that this research was supported by Czech Health Research Council grant (ref. NV18-04-00159), Ministry of Health of the Czech Republic (ref. 00098892). TR, MD, and MK report that this research was supported by Czech Health Research Council grant (ref. NV18-04-00159) and Ministry of Health of the Czech Republic (ref. 65269705). EK reports that this research was supported by Czech Health Research Council grant (ref. NV18-04-00159). PB received funding from the European Union Horizon 2020 research and innovation program under Marie Skłodowska-Curie grant agreement (No. 846793), and by a NARSAD Young Investigator Grant from the Brain and Behavior Research Foundation (No. 27238) for duration of this project. AS received funding from the European Union Horizon 2020 research and innovation program under Marie Skłodowska-Curie grant agreement (No. 794986) for the duration of this project. The authors have no other conflicts of interest to declare.

Ethical Statement: The authors are accountable for all aspects of the work in ensuring that questions related to the accuracy or integrity of any part of the work are appropriately investigated and resolved. The study was conducted in accordance with the Declaration of Helsinki (as revised in 2013). The study was approved by institutional ethics board of University Hospital Brno (No. EKV-2017-055) and informed consent was taken from all individual participants.

References

1. Smith SS, Stewart ME, Davies BM, Kotter MRN. The Prevalence of Asymptomatic and Symptomatic Spinal Cord Compression on Magnetic Resonance Imaging: A Systematic Review and Meta-analysis. Global Spine J 2021;11:597-607.
2. Kovalova I, Kerkovsky M, Kadanka Z, Kadanka Z Jr, Nemec M, Jurova B, Dusek L, Jarkovsky J, Bednarik J. Prevalence and Imaging Characteristics of Nonmyelopathic and Myelopathic Spondylotic Cervical Cord Compression. Spine (Phila Pa 1976) 2016;41:1908-16.
3. Nouri A, Tetreault L, Singh A, Karadimas SK, Fehlings MG. Degenerative Cervical Myelopathy: Epidemiology, Genetics, and Pathogenesis. Spine (Phila Pa 1976) 2015;40:E675-93.
4. Martin AR, De Leener B, Cohen-Adad J, Cadotte DW, Nouri A, Wilson JR, Tetreault L, Crawley AP, Mikulis DJ, Ginsberg H, Fehlings MG. Can microstructural MRI detect subclinical tissue injury in subjects with asymptomatic cervical spinal cord compression? A prospective cohort study. BMJ Open 2018;8:e019809.
5. Kerkovský M, Bednarík J, Dušek L, Sprláková-Puková A, Urbánek I, Mechl M, Válek V, Kadanka Z. Magnetic resonance diffusion tensor imaging in patients with cervical spondylotic spinal cord compression: correlations between clinical and electrophysiological findings. Spine (Phila Pa 1976) 2012;37:48-56.
6. Martin AR, De Leener B, Cohen-Adad J, Cadotte DW, Kalsi-Ryan S, Lange SF, Tetreault L, Nouri A, Crawley A, Mikulis DJ, Ginsberg H, Fehlings MG. A Novel MRI Biomarker of Spinal Cord White Matter Injury: T2*-Weighted White Matter to Gray Matter Signal Intensity Ratio. AJNR Am J Neuroradiol 2017;38:1266-73.
7. Labounek R, Valošek J, Horák T, Svátková A, Bednařík P, Vojtíšek L, Horáková M, Nestrašil I, Lenglet C, Cohen-Adad J, Bednařík J, Hluštík P. HARDI-ZOOMit protocol improves specificity to microstructural changes in presymptomatic myelopathy. Sci Rep 2020;10:17529.
8. Horak T, Horakova M, Svatkova A, Kadanka Z, Kudlicka P, Valosek J, Rohan T, Kerkovsky M, Vlckova E, Kadanka Z, Deelchand DK, Henry PG, Bednarik J, Bednarik P. In vivo Molecular Signatures of Cervical Spinal Cord Pathology in Degenerative Compression. J Neurotrauma 2021;38:2999-3010.
9. Kadanka Z Jr, Adamova B, Kerkovsky M, Kadanka Z, Dusek L, Jurova B, Vlckova E, Bednarik J. Predictors of symptomatic myelopathy in degenerative cervical spinal cord compression. Brain Behav 2017;7:e00797.
10. Yue WM, Tan SB, Tan MH, Koh DC, Tan CT. The Torg--Pavlov ratio in cervical spondylotic myelopathy: a comparative study between patients with cervical spondylotic myelopathy and a nonspondylotic, nonmyelopathic population. Spine (Phila Pa 1976) 2001;26:1760-4.
11. Bednarik J, Kadanka Z, Dusek L, Kerkovsky M, Vohanka S,

Novotny O, Urbanek I, Kratochvilova D. Presymptomatic spondylotic cervical myelopathy: an updated predictive model. Eur Spine J 2008;17:421-31.
12. Wilson JR, Barry S, Fischer DJ, Skelly AC, Arnold PM, Riew KD, Shaffrey CI, Traynelis VC, Fehlings MG. Frequency, timing, and predictors of neurological dysfunction in the nonmyelopathic patient with cervical spinal cord compression, canal stenosis, and/or ossification of the posterior longitudinal ligament. Spine (Phila Pa 1976) 2013;38:S37-54.
13. De Leener B, Lévy S, Dupont SM, Fonov VS, Stikov N, Louis Collins D, Callot V, Cohen-Adad J. SCT: Spinal Cord Toolbox, an open-source software for processing spinal cord MRI data. Neuroimage 2017;145:24-43.
14. Gros C, De Leener B, Badji A, Maranzano J, Eden D, Dupont SM, et al. Automatic segmentation of the spinal cord and intramedullary multiple sclerosis lesions with convolutional neural networks. Neuroimage 2019;184:901-15.
15. Valošek J, Labounek R, Horák T, Horáková M, Bednařík P, Keřkovský M, Kočica J, Rohan T, Lenglet C, Cohen-Adad J, Hluštík P, Vlčková E, Kadaňka Z Jr, Bednařík J, Svatkova A. Diffusion magnetic resonance imaging reveals tract-specific microstructural correlates of electrophysiological impairments in non-myelopathic and myelopathic spinal cord compression. Eur J Neurol 2021;28:3784-97.
16. Papinutto N, Henry RG. Evaluation of Intra- and Interscanner Reliability of MRI Protocols for Spinal Cord Gray Matter and Total Cross-Sectional Area Measurements. J Magn Reson Imaging 2019;49:1078-90.
17. Ost K, Jacobs WB, Evaniew N, Cohen-Adad J, Anderson D, Cadotte DW. Spinal Cord Morphology in Degenerative Cervical Myelopathy Patients; Assessing Key Morphological Characteristics Using Machine Vision Tools. J Clin Med 2021;10:892.
18. Seif M, David G, Huber E, Vallotton K, Curt A, Freund P. Cervical Cord Neurodegeneration in Traumatic and Non-Traumatic Spinal Cord Injury. J Neurotrauma 2020;37:860-7.
19. Martin AR, De Leener B, Cohen-Adad J, Kalsi-Ryan S, Cadotte DW, Wilson JR, Tetreault L, Nouri A, Crawley A, Mikulis DJ, Ginsberg H, Massicotte EM, Fehlings MG. Monitoring for myelopathic progression with multiparametric quantitative MRI. PLoS One 2018;13:e0195733.
20. Grabher P, Mohammadi S, Trachsler A, Friedl S, David G, Sutter R, Weiskopf N, Thompson AJ, Curt A, Freund P. Voxel-based analysis of grey and white matter degeneration in cervical spondylotic myelopathy. Sci Rep 2016;6:24636.
21. Cohen-Adad J, Alonso-Ortiz E, Abramovic M, Arneitz C, Atcheson N, Barlow L, et al. Generic acquisition protocol for quantitative MRI of the spinal cord. Nat Protoc 2021;16:4611-32.

Cite this article as: Horáková M, Horák T, Valošek J, Rohan T, Koriťáková E, Dostál M, Kočica J, Skutil T, Keřkovský M, Kadaňka Z Jr, Bednařík P, Svátková A, Hluštík P, Bednařík J. Semi-automated detection of cervical spinal cord compression with the Spinal Cord Toolbox. Quant Imaging Med Surg 2022;12(4):2261-2279. doi: 10.21037/qims-21-782

Supplementary

Torsion calculation

The ROC analysis with AUC (95% CI) for each variant of torsion calculation appears in *Table S1*. Using two slices and three slices above and below provided very similar results, with the latter variant proving slightly better in terms of average area under the curve (AUC). The only worse AUC value was at C3/4 level, with the lowest number of compressions. This study therefore employed variant with three slices above and below.

Table S1 Comparison of AUC (95% CI) in various approaches to torsion calculation (with angle correction)

	Torsion v1	Torsion v2	Torsion v3
C3/4	0.737 (0.600, 0.873)	0.772 (0.647, 0.897)	0.737 (0.607, 0.868)
C4/5	0.696 (0.606, 0.786)	0.762 (0.679, 0.844)	0.764 (0.683, 0.844)
C5/6	0.661 (0.575, 0.746)	0.748 (0.671, 0.824)	0.774 (0.701, 0.847)
C6/7	0.633 (0.526, 0.741)	0.694 (0.587, 0.801)	0.719 (0.615, 0.824)

Angle correction

The differences between SCT-derived parameters with and without angle correction in HC and levels with compression appear in *Table S2*. The difference was defined as uncorrected minus corrected. The difference was significant in almost all parameters and all levels, except CR (and eccentricity) and torsion. In accord with the anatomical curvature of the spine, the greatest differences between corrected and uncorrected values appeared in AP diameter (and subsequently in CR and eccentricity), as well as in CSA at levels C3/4 and C6/7. Repeated measures ANOVA found no difference between levels in RL and solidity, although there were differences in AP, CR, CSA, eccentricity, and torsion.

https://dx.doi.org/10.21037/qims-21-782

Table S2 Differences between parameters extracted with and without angle correction for HC and levels with compressions in SCC

		Healthy controls	P value	Levels with compressions	P value
RL (mm)					
	C3/4	0.02 (0, 0.06)	<0.0005	0.04 (0, 0.22)	<0.0005
	C4/5	0.02 (0, 0.06)	<0.0005	0.02 (0, 0.11)	<0.0005
	C5/6	0.02 (0, 0.07)	<0.0005	0.02 (0, 0.09)	<0.0005
	C6/7	0.02 (-0.01, 0.07)	<0.0005	0.02 (0, 0.10)	<0.0005
AP (mm)					
	C3/4	0.06 (0, 0.33)	<0.0005	0.04 (0, 0.26)	<0.0005
	C4/5	0.01 (0, 0.07)	<0.0005	0.01 (0, 0.10)	<0.0005
	C5/6	0.01 (0, 0.08)	<0.0005	0.01 (0, 0.10)	<0.0005
	C6/7	0.08 (0, 0.56)	<0.0005	0.02 (0, 0.26)	<0.0005
CR (%)					
	C3/4	0.44 (-0.11, 2.47)	<0.0005	0.12 (-0.73, 1.88)	0.051
	C4/5	-0.01 (-0.19, 0.49)	0.140	0.00 (-0.39, 0.66)	0.164
	C5/6	0.00 (-0.11, 0.63)	<0.0005	0.00 (-0.22, 0.69)	0.032
	C6/7	0.54 (-0.03, 4.8)	<0.0005	0.03 (-0.29, 1.79)	0.003
CSA (mm^2)					
	C3/4	0.63 (0.04, 2.84)	<0.0005	0.41 (0.02, 2.48)	<0.0005
	C4/5	0.12 (0.02, 0.65)	<0.0005	0.14 (0.02, 1.09)	<0.0005
	C5/6	0.23 (0.01, 1.2)	<0.0005	0.14 (0.01, 1.02)	<0.0005
	C6/7	0.81 (0.05, 5.11)	<0.0005	0.24 (0.00, 2.65)	<0.0005
Solidity (%)					
	C3/4	-0.44 (-1.1, -0.06)	<0.0005	-0.60 (-1.60, -0.20)	<0.0005
	C4/5	-0.39 (-0.96, 0.01)	<0.0005	-0.45 (-1.22, -0.05)	<0.0005
	C5/6	-0.44 (-0.89, 0.00)	<0.0005	-0.55 (-1.14, -0.05)	<0.0005
	C6/7	-0.43 (-1.48, -0.02)	<0.0005	-0.50 (-1.33, 0.00)	<0.0005
Torsion (degree)					
	C3/4	0.02 (-0.06, 0.10)	0.001	0.00 (-0.07, 0.29)	0.230
	C4/5	0.00 (-0.05, 0.05)	0.517	0.00 (-0.04, 0.09)	0.791
	C5/6	0.00 (-0.04, 0.12)	0.343	0.00 (-0.06, 0.07)	0.767
	C6/7	0.03 (-0.05, 0.47)	<0.0005	0.00 (-0.05, 0.21)	0.285

The P values represent the significance of paired *t*-test (RL, AP, CR, CSA,) and Wilcoxon signed ranks test (solidity, torsion).

https://dx.doi.org/10.21037/qims-21-782

There was almost no difference in ROC analyses of compression detection based on values without and with angle correction, respectively (average AUC was 0.858 *vs*. 0.853 for C3/4, 0.794 *vs* 0.792 for C4/5, 0.783 *vs*. 0.780 for C5/6 and 0.772 *vs*. 0.774 for C6/7).

Relationship between eccentricity and CR

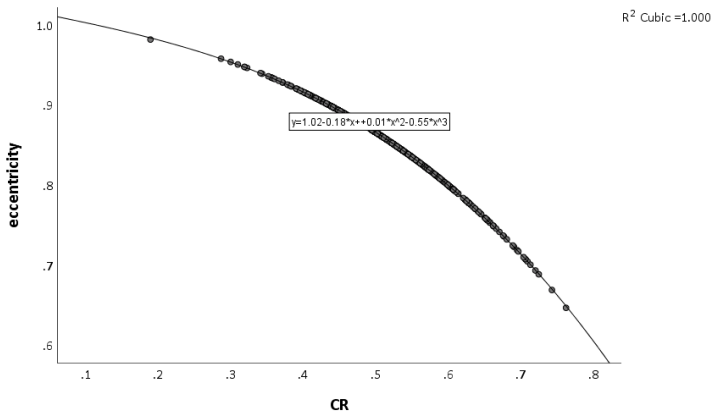

Figure S1 The relationship between eccentricity and CR is cubic, with $R^{2=1}$.

https://dx.doi.org/10.21037/qims-21-782

Normative data using values without angle correction

Table S3 Normative data of parameters without angle correction, compression characteristics, and proposed cut-offs based on ROC analysis

	Healthy controls	Levels with compressions	Cut-off	AUC (95% CI)	Sensitivity	Specificity
RL (mm)						
C3/4	12.6±1.1	13.2±1.2				
C4/5	13.3±1.1	13.8±1.2				
C5/6	13.2±1.1	13.3±1.5				
C6/7	12.2±1.2	12.3±1.1				
AP (mm)						
C3/4	7.4±0.5	6.1±0.8				
C4/5	7.3±0.6	6.2±0.8				
C5/6	7.0±0.6	6.1±0.8				
C6/7	6.7±0.6	5.7±0.6				
CR (%)						
C3/4	59.3±6.4	46.3±6.2	52.4	0.944 (0.898, 0.990)	87.5	87.9
C4/5	55.1±6.4	45.8±6.8	51.5	0.850 (0.786, 0.915)	83.1	74.2
C5/6	53.5±6.3	46.2±6.6	49.6	0.793 (0.724, 0.862)	68.5	77.3
C6/7	55.8±6.6	47.0±5.7	51.1	0.849 (0.776, 0.922)	83.3	75.8
CSA (mm^2)						
C3/4	72.6±8.2	60.1±10.9	66.7	0.883 (0.794, 0.971)	87.5	81.8
C4/5	75.6±8.6	64.6±10.0	69.2	0.806 (0.731, 0.882)	73.8	80.3
C5/6	71.8±9.5	61.0±10.8	61.1	0.779 (0.707, 0.850)	55.1	90.9
C6/7	63.7±9.5	53.9±8.5	57.2	0.786 (0.696, 0.877)	71.4	78.8
Solidity (%)						
C3/4	96.3 (94.2, 97.8)	93.7 (87.9, 96.8)	95.2	0.877 (0.784, 0.970)	79.2	89.4
C4/5	96.0 (93.7, 97.4)	94.3 (87.3, 97.2)	94.6	0.754 (0.669, 0.839)	60.0	86.4
C5/6	95.9 (93.4, 97.7)	93.9 (85.1, 97.0)	94.2	0.794 (0.725, 0.863)	58.4	89.4
C6/7	95.6 (93.2, 98.1)	94.4 (90.6, 97.0)	94.6	0.748 (0.652, 0.844)	66.7	74.2
Torsion (degree)						
C3/4	0.84 (0.45, 1.99)	1.48 (0.53, 3.81)	1.33	0.729 (0.598, 0.861)	58.3	87.9
C4/5	0.70 (0.26, 1.60)	1.25 (0.49, 2.86)	0.94	0.764 (0.683, 0.844)	72.3	72.7
C5/6	0.91 (0.44, 1.69)	1.33 (0.58, 3.17)	1.12	0.766 (0.691, 0.841)	74.2	71.2
C6/7	1.22 (0.53, 2.82)	2.12 (0.58, 3.89)	2.10	0.704 (0.599, 0.810)	52.4	86.4

Data are presented as mean ± SD where normally distributed, median (5th–95th percentile) for data without normal distribution. The values were calculated from 66 HC, 24 compressions at C3/4 level, 65 at C4/5, 89 at C5/6 and 42 at C6/7.

https://dx.doi.org/10.21037/qims-21-782

Compression detection using values without angle correction

Table S4 Models for automated compression detection employing morphometric parameters without angle correction

	Coefficients	OR (95% CI)	p-value (factors)	p-value (model)	Nagelkerke R^2	AUC (95% CI) of predicted probabilities
C3/4				<0.0005	0.848	0.978 (0.948, 1.000)
Constant	71.339		0.061			
CR (%)	-0.462	0.630 (0.457, 0.869)	0.005			
CSA (mm^2)	-0.174	0.841 (0.713, 0.991)	0.038			
Solidity (%)	-0.399	0.671 (0.312, 1.445)	0.308			
Torsion (degree)	2.128	8.399 (0.354, 199.542)	0.188			
C4/5				<0.0005	0.723	0.943 (0.904, 0.981)
Constant	51.939		0.003			
CR (%)	-0.272	0.762 (0.670, 0.867)	<0.0005			
CSA (mm^2)	-0.100	0.904 (0.839, 0.975)	0.009			
Solidity (%)	-0.356	0.701 (0.491, 1.000)	0.050			
Torsion (degree)	2.679	14.566 (3.716, 57.098)	<0.0005			
C5/6				<0.0005	0.712	0.940 (0.905, 0.976)
Constant	70.725		0.001			
CR (%)	-0.190	0.827 (0.740, 0.924)	0.001			
CSA (mm^2)	-0.069	0.934 (0.881, 0.989)	0.020			
Solidity (%)	-0.633	0.531 (0.344, 0.819)	0.004			
Torsion (degree)	3.385	29.517 (6.832, 127.519)	<0.0005			
C6/7				<0.0005	0.800	0.964 (0.931, 0.997)
Constant	85.839		0.002			
CR (%)	-0.427	0.653 (0.54, 0.79)	<0.0005			
CSA (mm^2)	-0.171	0.843 (0.763, 0.931)	0.001			
Solidity (%)	-0.606	0.546 (0.321, 0.926)	0.025			
Torsion (degree)	1.869	6.482 (2.302, 18.248)	<0.0005			
Pooled model				<0.0005	0.740	0.948 (0.930, 0.967)
Constant	57.679		<0.0005			
CR (%)	-0.269	0.764 (0.716, 0.816)	<0.0005			
CSA (mm^2)	-0.099	0.906 (0.871, 0.941)	<0.0005			
Solidity (%)	-0.443	0.642 (0.517, 0.798)	<0.0005			
Torsion (degree)	2.088	8.072 (4.484, 14.531)	<0.0005			
Level C6/7 (yes or no)	-2.603	0.074 (0.030, 0.183)	<0.0005			

Models were constructed over data from HC and from levels with compression in SCC.

https://dx.doi.org/10.21037/qims-21-782

Cross-validation of the pooled model

The cross-validation of the pooled model was performed by constructing 6 models, each over 5/6 of the data from levels with compression and levels in healthy controls, ROC analysis with definition of the best cut-off for predicted probability employing the Youden index and then calculating the probability, and consequently sensitivity and specificity of compression detection, in the remaining 1/6 of participants. The results appear in *Table S5*. The overall sensitivity of compression detection in participants that were not used for model construction was 0.836, specificity 0.905, positive predictive value 0.880 and negative predictive value 0.869. *Table S-5* also shows very similar coefficients for each of the six models, suggesting great stability for the model predictions.

Table S5 Cross validation of compression detection. Each of the six models was constructed over 5/6 of data and the remaining 1/6 of data was used to calculate sensitivity and specificity of compression detection using the predicted probability acquired from that model

	Coefficients	OR (95% CI)	P value (factors)	P value (model)	Nagelkerke R^2	AUC (95% CI) of predicted probabilities
Model 1				<0.0005	0.727	0.944 (0.923, 0.966)
Constant	57.806		<0.0005			
CR (%)	-0.262	0.77 (0.716, 0.827)	<0.0005			Cut-off: 0.465
CSA (mm^2)	-0.103	0.903 (0.866, 0.941)	<0.0005			Sensitivity: 0.917
Solidity (%)	-0.416	0.66 (0.517, 0.842)	0.001			Specificity: 0.886
Torsion (degree)	2.110	8.244 (4.398, 15.455)	<0.0005			
C67	-2.742	0.064 (0.024, 0.171)	<0.0005			
Model 2				<0.0005	0.718	0.941 (0.919, 0.963)
Constant	48.626		<0.0005			
CR (%)	-0.257	0.773 (0.722, 0.828)	<0.0005			Cut-off: 0.491
CSA (mm^2)	-0.095	0.909 (0.874, 0.946)	<0.0005			Sensitivity: 0.919
Solidity (%)	-0.331	0.718 (0.573, 0.9)	0.004			Specificity:0.886
Torsion (degree)	2.330	10.277 (5.287, 19.976)	<0.0005			
C67	-2.506	0.082 (0.032, 0.208)	<0.0005			
Model 3				<0.0005	0.772	0.958 (0.941, 0.976)
Constant	72.581		<0.0005			
CR (%)	-0.308	0.735 (0.676, 0.798)	<0.0005			Cut-off: 0.485
CSA (mm^2)	-0.090	0.914 (0.875, 0.955)	<0.0005			Sensitivity: 0676
Solidity (%)	-0.559	0.572 (0.442, 0.739)	<0.0005			Specificity: 0.932
Torsion (degree)	2.341	10.392 (5.082, 21.252)	<0.0005			
C67	-2.715	0.066 (0.024, 0.185)	<0.0005			
Model 4				<0.0005	0.713	0.94 (0.918, 0.962)
Constant	48.811		<0.0005			
CR (%)	-0.266	0.766 (0.715, 0.822)	<0.0005			Cut-off: 0.466
CSA (mm^2)	-0.094	0.91 (0.872, 0.949)	<0.0005			Sensitivity:0.89

Table S5 (*continued*)

https://dx.doi.org/10.21037/qims-21-782

Table S5 (*continued*)

	Coefficients	OR (95% CI)	P value (factors)	P value (model)	Nagelkerke R^2	AUC (95% CI) of predicted probabilities
Solidity (%)	-0.326	0.722 (0.577, 0.903)	0.004			Specificity: 0.932
Torsion (degree)	2.102	8.183 (4.362, 15.352)	<0.0005			
C67	-2.805	0.06 (0.022, 0.165)	<0.0005			
Model 5				<0.0005	0.748	0.95 (0.931, 0.97)
Constant	56.316		<0.0005			
CR (%)	-0.289	0.749 (0.695, 0.807)	<0.0005			Cut-off: 0.569
CSA (mm^2)	-0.110	0.896 (0.856, 0.938)	<0.0005			Sensitivity: 0.784
Solidity (%)	-0.382	0.682 (0.537, 0.867)	0.002			Specificity: 0.886
Torsion (degree)	2.248	9.467 (4.693, 19.096)	<0.0005			
C67	-2.870	0.057 (0.02, 0.162)	<0.0005			
Model 6				<0.0005	0.747	0.949 (0.929, 0.969)
Constant	64.598		<0.0005			
CR (%)	-0.271	0.763 (0.709, 0.821)	<0.0005			Cut-off: 0.486
CSA (mm^2)	-0.126	0.881 (0.842, 0.923)	<0.0005			Sensitivity: 0.833
Solidity (%)	-0.465	0.628 (0.49, 0.805)	<0.0005			Specificity: 0.909
Torsion (degree)	2.028	7.602 (4.013, 14.402)	<0.0005			
C67	-2.825	0.059 (0.021, 0.164)	<0.0005			

Compression detection including levels without compression in SCC group

The results are summarized in *Table S-6*. Importantly, the variables in *Table S6* are analogous to *Table 3* in the main text, even though not all variables were significant and some of them did not remain after backward stepwise removal of factors. In particular, CSA was not significant at levels C3/4 and C4/5, solidity was not significant at C3/4 and C6/7 and further, height was significant at level C5/6, although the OR was very close to 1 (OR =1.031 with 95% CI: 1.008–1.055). Also presented are two pooled models, one analogous to the pooled model in the main text and the second with the addition of another variable – level C3/4, which proved significant at OR = 0.262.

Table S6 The models are constructed from parameters with angle correction, over 24 compressions and 160 non-compressions at level C3/4, 65 compressions and 119 non-compressions at level C4/5, 89 compressions and 95 non-compressions at level C5/6, 42 compressions and 142 non-compressions at level C6/7 and 220 compressions and 516 non-compressions in pooled models

	Coefficients	OR (95% CI)	p-value (factors)	p-value (model)	Nagelkerke R^2	AUC (95% CI) of predicted probabilities
C3/4				<0.0005	0.550	0.915 (0.860, 0.970)
Constant	38.357		0.017			
CR (%)	-0.211	0.81 (0.712, 0.921)	0.001			
CSA (mm^2)	-0.040	0.961 (0.886, 1.042)	0.335			
Solidity (%)	-0.296	0.744 (0.52, 1.064)	0.105			
Torsion (degree)	1.166	3.208 (1.436, 7.167)	0.004			

Table S6 (*continued*)

https://dx.doi.org/10.21037/qims-21-782

Table S6 (*continued*)

	Coefficients	OR (95% CI)	p-value (factors)	p-value (model)	Nagelkerke R^2	AUC (95% CI) of predicted probabilities
C4/5				<0.0005	0.494	0.868 (0.815, 0.921)
Constant	33.392		0.003			
CR (%)	-0.197	0.821 (0.753, 0.896)	<0.0005			
CSA (mm^2)	-0.024	0.976 (0.933, 1.021)	0.286			
Solidity (%)	-0.252	0.777 (0.612, 0.987)	0.039			
Torsion (degree)	1.413	4.109 (1.897, 8.899)	<0.0005			
C5/6				<0.0005	0.545	0.888 (0.840, 0.935)
Constant	38.425		0.002			
CR (%)	-0.134	0.875 (0.808, 0.947)	0.001			
CSA (mm^2)	-0.059	0.943 (0.903, 0.984)	0.008			
Solidity (%)	-0.316	0.729 (0.558, 0.954)	0.021			
Torsion (degree)	1.651	5.211 (2.406, 11.285)	<0.0005			
C6/7				<0.0005	0.558	0.913 (0.869, 0.957)
Constant	32.639		0.046			
CR (%)	-0.231	0.794 (0.721, 0.874)	<0.0005			
CSA (mm^2)	-0.114	0.892 (0.836, 0.952)	0.001			
Solidity (%)	-0.188	0.829 (0.590, 1.164)	0.279			
Torsion (degree)	1.253	3.502 (1.879, 6.530)	<0.0005			
Pooled model (analogous)				<0.0005	0.551	0.896 (0.872, 0.920)
Constant	34.947		<0.0005			
CR (%)	-0.198	0.820 (0.784, 0.858)	<0.0005			
CSA (mm^2)	-0.049	0.952 (0.928, 0.976)	<0.0005			
Solidity (%)	-0.252	0.778 (0.678, 0.892)	<0.0005			
Torsion (degree)	1.309	3.702 (2.609, 5.254)	<0.0005			
Level C6/7	-1.584	0.205 (0.114, 0.370)	<0.0005			
Pooled model (with C3/4)				<0.0005	0.573	0.904 (0.881, 0.926)
Constant	35.589		<0.0005			
CR (%)	-0.182	0.833 (0.796, 0.872)	<0.0005			
CSA (mm^2)	-0.055	0.947 (0.923, 0.971)	<0.0005			
Solidity (%)	-0.259	0.772 (0.670, 0.888)	<0.0005			
Torsion (degree)	1.280	3.595 (2.549, 5.072)	<0.0005			
Level C3/4	-1.341	0.262 (0.136, 0.502)	<0.0005			
Level C6/7	-1.917	0.147 (0.080, 0.272)	<0.0005			

#Analysis of DCM group

https://dx.doi.org/10.21037/qims-21-782

Analysis of DCM group

Table S7 Analysis of levels with compression in asymptomatic (NMDC) and symptomatic (DCM) participants for parameters extracted with SCT with angle correction

	NMDC	DCM	P value (MW-test)	AUC (95% CI)
CR (%)				
C3/4	47.0±5.8	42.4±7.4	0.214	0.684 (0.402, 0.966)
C4/5	45.6±5.8	46.0±11.4	0.344	0.405 (0.191, 0.620)
C5/6	46.4±6.5	44.4±6.2	0.335	0.584 (0.432, 0.736)
C6/7	46.3±5.6	50.7±3.7	0.136	0.239 (0.029, 0.449)
CSA (mm^2)				
C3/4	62.7±7.8	47.1±13.7	0.017*	0.853 (0.653, 1.000)
C4/5	65.5±10.1	58.0±7.1	0.011*	0.753 (0.613, 0.892)
C5/6	61.6±10.8	55.1±8.5	0.058	0.665 (0.528, 0.802)
C6/7	53.4±8.2	53.0±9.8	0.942	0.513 (0.128, 0.898)
Solidity (%)				
C3/4	94.4±2.6	91.9±2.8	0.082	0.758 (0.502, 1.000)
C4/5	93.9±3.2	94.8±2.2	0.456	0.425 (0.243, 0.608)
C5/6	93.6±3.7	94.6±1.4	0.754	0.473 (0.338, 0.607)
C6/7	94.5±2.9	93.9±2.2	0.574	0.598 (0.271, 0.926)
Torsion (degree)				
C3/4	1.7±1.1	1.8±0.9	0.836	0.537 (0.265, 0.809)
C4/5	1.7±2.8	1.3±0.6	0.785	0.473 (0.284, 0.662)
C5/6	1.5±0.7	1.4±0.6	0.515	0.443 (0.262, 0.624)
C6/7	2.0±1.0	2.8±1.5	0.272	0.692 (0.294, 1.000)
Predicted probability				
C3/4	0.965 (0.068, 1.000)	0.997 (0.698, 1.000)	0.095	0.747 (0.513, 0.982)
C4/5	0.901 (0.074, 1.000)	0.866 (0.484, 1.000)	0.757	0.469 (0.280, 0.659)
C5/6	0.963 (0.220, 1.000)	0.981 (0.764, 1.000)	0.546	0.553 (0.410, 0.696)
C6/7	0.898 (0.220, 1.000)	0.968 (0.709, 0.968)	0.510	0.615 (0.308, 0.923)

Data are presented as mean ± SD where normally distributed, median (5th–95th percentile) for data without normal distribution. The values for NMDC group are calculated from 19 compressions at C3/4 level, 55 at C4/5 level, 76 at C5/6 level and 39 at C6/7 level. The values for DCM group are calculated from 5 compressions at C3/4 level, 10 at C4/5 level, 13 at C5/6 level and 3 at C6/7 level. Mann-Whitney test was used to compare NMDC and DCM groups (because of the small number of observations in each group). ROC analysis was performed to analyse the ability of quantitative parameters and predicted probability to distinguish between compressions in NMDC and DCM group. AUC, area under curve; CI, confidence interval; RL, right-left diameter; AP, anterior-posterior diameter; CR, compressive ratio; CSA, cross-sectional area. *P<0.05.

https://dx.doi.org/10.21037/qims-21-782

Inter-trial variability of morphometric parameters divided into HC and SCC

Table S8 Differences in morphometric parameters between the two MRI examinations in HC and SCC

HC	SCT (n=35)	SCT (with correction)	Rater 1	Rater 2	Rater 3
RL (mm)					
C3/4	0.50 (-0.45, 0.93)	0.47 (-0.45, 0.93)	1.20 (0.38, 1.88)	0.36 (-0.49, 1.29)	0.83 (-0.23, 1.64)
C4/5	0.52 (-0.58, 1.07)	0.47 (-0.56, 1.02)	1.00 (0.28, 1.54)	0.24 (-0.56, 1.06)	0.70 (-0.46, 2.01)
C5/6	0.45 (-0.17, 1.03)	0.42 (-0.16, 1.01)	0.90 (0.20, 1.76)	0.30 (-0.63, 0.98)	0.62 (-0.43, 3.21)
C6/7	0.44 (-0.18, 1.3)	0.45 (-0.18, 1.29)	0.80 (-0.26, 2.88)	0.18 (-0.65, 0.91)	0.60 (-0.46, 4.13)
ICC	0.884 (0.321, 0.960)	0.886 (0.321, 0.961)	0.620 (-0.081, 0.870)	0.873 (0.745, 0.928)	0.569 (0.110, 0.776)
AP (mm)					
C3/4	0.58 (-0.29, 1.05)	0.59 (-0.28, 1.07)	1.30 (0.30, 2.04)	0.5 (-0.51, 1.07)	0.83 (-0.27, 2.10)
C4/5	0.28 (-0.26, 0.91)	0.32 (-0.28, 0.92)	1.30 (0.60, 1.92)	0.45 (-0.33, 1.27)	1.00 (0.42, 2.17)
C5/6	0.35 (-0.40, 1.01)	0.31 (-0.40, 0.98)	1.20 (0.66, 2.00)	0.51 (-0.27, 1.25)	0.78 (0.05, 1.80)
C6/7	0.51 (-0.19, 1.35)	0.44 (-0.23, 0.97)	1.10 (0.40, 2.20)	0.53 (-0.71, 1.35)	0.79 (0.13, 3.04)
ICC	0.685 (0.078, 0.867)	0.721 (0.130, 0.878)	0.273 (-0.049, 0.633)	0.613 (0.104, 0.813)	0.332 (-0.099, 0.644)
CR (%)					
C3/4	2.66 (-4.10, 6.23)	2.68 (-3.58, 5.77)	5.95 (0.49, 10.56)	1.49 (-4.23, 5.45)	2.68 (-3.53, 13.08)
C4/5	0.86 (-6.21, 4.25)	0.84 (-6.57, 4.24)	6.72 (1.15, 11.43)	2.86 (-2.94, 7.07)	4.58 (-0.62, 17.29)
C5/6	0.75 (-5.53, 6.68)	0.66 (-5.62, 6.45)	5.58 (2.09, 10.60)	3.24 (-3.66, 8.71)	3.38 (-4.00, 14.83)
C6/7	2.03 (-3.80, 10.65)	1.12 (-4.49, 7.21)	7.09 (-0.46, 15.33)	3.02 (-3.76, 12.56)	3.98 (-7.85, 20.41)
ICC	0.827 (0.734, 0.884)	0.841 (0.767, 0.890)	0.538 (-0.088, 0.826)	0.775 (0.481, 0.884)	0.565 (0.206, 0.749)
CSA (mm^2)					
C3/4	7.8 (-5.5, 13.8)	8.4 (-5.6, 14.0)	15.0 (8.0, 29.0)	5.0 (-4.0, 16.0)	13.0 (1.4, 23.8)
C4/5	6.0 (-5.5, 13.3)	6.3 (-5.5, 13.2)	16.0 (4.6, 22.4)	6.0 (-4.2, 16.0)	14.0 (5.8, 30.2)
C5/6	5.9 (-3.4, 13.0)	5.8 (-3.7, 12.8)	14.0 (5.0, 24.4)	5.0 (-2.4, 16.4)	12.0 (5.8, 30.0)
C6/7	7.7 (-3.0, 14.0)	6.0 (-2.1, 12.8)	13.0 (3.0, 35.7)	5.0 (-8.8, 14.6)	13.0 (4.6, 52.9)
ICC	0.757 (0.004, 0.916)	0.778 (0.048, 0.922)	0.347 (-0.076, 0.694)	0.713 (0.246, 0.867)	0.319 (-0.098, 0.640)
Solidity (%)					
C3/4	-0.06 (-3.20, 3.27)	-0.15 (-3.30, 2.30)			
C4/5	-0.32 (-3.99, 1.51)	-0.52 (-3.90, 1.98)			
C5/6	-0.75 (-3.50, 2.45)	-0.94 (-3.48, 2.48)			
C6/7	-0.15 (-3.93, 3.61)	-0.35 (-4.00, 3.28)			
ICC	-0.040 (-0.121, 0.200)	0.005 (-0.151, 0.163)			
SCC	n=30				
RL (mm)					
C3/4	0.52 (-0.34, 1.62)	0.53 (-0.37, 1.65)	0.90 (0.21, 1.65)	0.32 (-1.02, 0.88)	0.58 (-0.12, 1.71)

Table S8 (*continued*)

https://dx.doi.org/10.21037/qims-21-782

Table S8 (*continued*)

HC	SCT (n=35)	SCT (with correction)	Rater 1	Rater 2	Rater 3
C4/5	0.75 (0.02, 2.00)	0.75 (0.03, 2.01)	1.00 (0.36, 2.23)	0.36 (-0.85, 1.55)	0.45 (-0.55, 3.10)
C5/6	0.51 (-1.05, 2.05)	0.51 (-1.05, 2.05)	0.45 (-2.54, 1.74)	-0.09 (-4.08, 1.46)	0.61 (-1.07, 1.88)
C6/7	0.65 (-0.38, 1.62)	0.63 (-0.38, 1.60)	0.80 (-0.29, 1.55)	0.28 (-1.03, 1.37)	0.53 (-2.12, 1.96)
ICC	0.781 (0.194, 0.914)	0.781 (0.193, 0.914)	0.699 (0.057, 0.879)	0.749 (0.658, 0.819)	0.683 (0.420, 0.815)
AP (mm)					
C3/4	0.60 (-0.46, 1.36)	0.54 (-0.48, 1.36)	1.45 (0.66, 2.2)	0.66 (-0.96, 1.68)	0.48 (-0.37, 1.66)
C4/5	0.25 (-0.23, 1.51)	0.22 (-0.22, 1.49)	1.05 (0.40, 2.13)	0.67 (-0.40, 1.35)	0.64 (-0.89, 1.68)
C5/6	0.38 (-0.28, 1.03)	0.35 (-0.28, 1.02)	0.90 (-0.45, 1.89)	0.07 (-1.56, 1.34)	0.45 (-1.85, 1.80)
C6/7	0.28 (-0.17, 1.62)	0.35 (-0.16, 1.38)	0.85 (0.01, 2.48)	0.27 (-0.54, 1.32)	0.42 (-1.27, 2.16)
ICC	0.659 (0.153, 0.841)	0.660 (0.140, 0.843)	0.388 (-0.085, 0.726)	0.669 (0.400, 0.806)	0.537 (0.281, 0.698)
CR (%)					
C3/4	1.69 (-5.65, 9.33)	1.48 (-5.55, 8.88)	7.48 (2.36, 13.18)	4.13 (-6.13, 11.27)	1.41 (-5.19, 9.87)
C4/5	0.21 (-6.38, 6.91)	0.13 (-6.38, 6.86)	4.58 (-0.92, 12.1)	3.19 (-4.34, 11.53)	0.01 (-6.25, 9.06)
C5/6	0.04 (-9.53, 7.91)	0.51 (-9.26, 8.00)	5.31 (-0.64, 13.41)	1.27 (-7.79, 11.25)	2.18 (-11.15, 12.19)
C6/7	-0.52 (-4.1, 10.39)	-0.42 (-4.08, 9.3)	6.75 (-2.63, 14.41)	1.47 (-5.69, 7.38)	0.59 (-6.37, 14.05)
ICC	0.819 (0.749, 0.871)	0.824 (0.756, 0.875)	0.650 (-0.071, 0.874)	0.802 (0.637, 0.883)	0.760 (0.667, 0.829)
CSA (mm^2)					
C3/4	9.2 (-6.5, 18.6)	8.0 (-6.4, 18.8)	16.0 (6.0, 23.5)	2.5 (-6.9, 11.5)	9.0 (-4.9, 21.3)
C4/5	6.4 (-2.1, 22.6)	6.6 (-2.2, 22.0)	12.5 (3.6, 29.5)	2.5 (-9.8, 13.5)	6.5 (-15.1, 33.3)
C5/6	7.5 (-5.1, 14.4)	7.0 (-5.0, 14.3)	10.5 (-4.5, 19.5)	0.5 (-27.1, 8.5)	4.5 (-16.4, 22.7)
C6/7	7.0 (-0.8, 19.5)	6.8 (-0.4, 17.6)	11.0 (-1.4, 24.3)	-3.5 (-12.5, 14.5)	4.5 (-20.1, 24.9)
ICC	0.636 (-0.006, 0.850)	0.639 (-0.009, 0.852)	0.381 (-0.097, 0.707)	0.691 (0.585, 0.774)	0.475 (0.241, 0.640)
Solidity (%)					
C3/4	-1.28 (-6.13, 1.72)	-1.41 (-6.11, 1.18)			
C4/5	-0.55 (-5.69, 1.82)	-0.59 (-5.72, 1.49)			
C5/6	-0.81 (-5.18, 2.81)	-0.61 (-4.87, 2.12)			
C6/7	-1.65 (-5.58, 2.66)	-1.55 (-4.98, 2.48)			
ICC	0.604 (0.379, 0.743)	0.623 (0.359, 0.769)			

Data are summarized as median (5th–95th percentile). ICCs (two-way random, absolute agreement, single measures) with 95% CI, comparing each parameter pooled per all intervertebral levels between the two MRI examinations ($p < 0.0005$).

https://dx.doi.org/10.21037/qims-21-782

Inter-trial and inter-rater variability of morphometric parameters (correlation matrices)

Table S9 Correlation matrices (Pearson correlation coefficients) of CR and CSA across all raters and SCT with and without angle correction

CR C3/4	SCT (1.5T)	SCTcor (1.5T)	SCT (3T)	SCTcor (3T)	Rater1 (1.5T)	Rater1 (3T)	Rater2 (1.5T)	Rater2 (3T)	Rater3 (1.5T)	Rater3 (3T)
SCT (1.5T)	1	0.994	0.861	0.844	0.907	0.859	0.909	0.849	0.825	0.841
SCTcor (1.5T)	0.994	1	0.872	0.859	0.905	0.870	0.907	0.862	0.825	0.849
SCT (3T)	0.861	0.872	1	0.992	0.837	0.855	0.850	0.843	0.738	0.872
SCTcor (3T)	0.844	0.859	0.992	1	0.835	0.843	0.839	0.824	0.732	0.860
Rater1 (1.5T)	0.907	0.905	0.837	0.835	1	0.885	0.921	0.843	0.862	0.836
Rater1 (3T)	0.859	0.870	0.855	0.843	0.885	1	0.876	0.912	0.792	0.932
Rater2 (1.5T)	0.909	0.907	0.850	0.839	0.921	0.876	1	0.840	0.779	0.815
Rater2 (3T)	0.849	0.862	0.843	0.824	0.843	0.912	0.840	1	0.792	0.914
Rater3 (1.5T)	0.825	0.825	0.738	0.732	0.862	0.792	0.779	0.792	1	0.773
Rater3 (3T)	0.841	0.849	0.872	0.860	0.836	0.932	0.815	0.914	0.773	1
CSA C3/4	SCT (1.5T)	SCTcor (1.5T)	SCT (3T)	SCTcor (3T)	Rater1 (1.5T)	Rater1 (3T)	Rater2 (1.5T)	Rater2 (3T)	Rater3 (1.5T)	Rater3 (3T)
SCT (1.5T)	1	0.997	0.808	0.805	0.851	0.776	0.831	0.758	0.639	0.777
SCTcor (1.5T)	0.997	1	0.802	0.802	0.842	0.769	0.819	0.758	0.638	0.777
SCT (3T)	0.808	0.802	1	0.996	0.781	0.747	0.758	0.732	0.712	0.759
SCTcor (3T)	0.805	0.802	0.996	1	0.774	0.740	0.750	0.725	0.723	0.750
Rater1 (1.5T)	0.851	0.842	0.781	0.774	1	0.788	0.816	0.781	0.567	0.715
Rater1 (3T)	0.776	0.769	0.747	0.740	0.788	1	0.815	0.785	0.615	0.841
Rater2 (1.5T)	0.831	0.819	0.758	0.750	0.816	0.815	1	0.836	0.695	0.802
Rater2 (3T)	0.758	0.758	0.732	0.725	0.781	0.785	0.836	1	0.595	0.833
Rater3 (1.5T)	0.639	0.638	0.712	0.723	0.567	0.615	0.695	0.595	1	0.721
Rater3 (3T)	0.777	0.777	0.759	0.750	0.715	0.841	0.802	0.833	0.721	1
CR C4/5	SCT (1.5T)	SCTcor (1.5T)	SCT (3T)	SCTcor (3T)	Rater1 (1.5T)	Rater1 (3T)	Rater2 (1.5T)	Rater2 (3T)	Rater3 (1.5T)	Rater3 (3T)
SCT (1.5T)	1	0.999	0.855	0.854	0.846	0.850	0.870	0.825	0.752	0.841
SCTcor (1.5T)	0.999	1	0.853	0.853	0.849	0.847	0.869	0.825	0.758	0.837
SCT (3T)	0.855	0.853	1	0.999	0.851	0.909	0.778	0.796	0.749	0.840
SCTcor (3T)	0.854	0.853	0.999	1	0.854	0.904	0.777	0.793	0.750	0.836
Rater1 (1.5T)	0.846	0.849	0.851	0.854	1	0.874	0.826	0.794	0.825	0.791
Rater1 (3T)	0.850	0.847	0.909	0.904	0.874	1	0.837	0.851	0.782	0.887
Rater2 (1.5T)	0.870	0.869	0.778	0.777	0.826	0.837	1	0.825	0.783	0.807
Rater2 (3T)	0.825	0.825	0.796	0.793	0.794	0.851	0.825	1	0.768	0.855
Rater3 (1.5T)	0.752	0.758	0.749	0.750	0.825	0.782	0.783	0.768	1	0.672
Rater3 (3T)	0.841	0.837	0.840	0.836	0.791	0.887	0.807	0.855	0.672	1

Table S9 (*continued*)

https://dx.doi.org/10.21037/qims-21-782

Table S9 (*continued*)

CSA C4/5	SCT (1.5T)	SCTcor (1.5T)	SCT (3T)	SCTcor (3T)	Rater1 (1.5T)	Rater1 (3T)	Rater2 (1.5T)	Rater2 (3T)	Rater3 (1.5T)	Rater3 (3T)
SCT (1.5T)	1	0.999	0.847	0.841	0.809	0.783	0.822	0.763	0.700	0.767
SCTcor (1.5T)	0.999	1	0.852	0.847	0.815	0.784	0.827	0.770	0.707	0.770
SCT (3T)	0.847	0.852	1	0.999	0.845	0.838	0.815	0.790	0.685	0.767
SCTcor (3T)	0.841	0.847	0.999	1	0.842	0.830	0.810	0.786	0.683	0.761
Rater1 (1.5T)	0.809	0.815	0.845	0.842	1	0.785	0.860	0.757	0.729	0.726
Rater1 (3T)	0.783	0.784	0.838	0.830	0.785	1	0.762	0.807	0.584	0.876
Rater2 (1.5T)	0.822	0.827	0.815	0.810	0.860	0.762	1	0.761	0.804	0.702
Rater2 (3T)	0.763	0.770	0.790	0.786	0.757	0.807	0.761	1	0.661	0.789
Rater3 (1.5T)	0.700	0.707	0.685	0.683	0.729	0.584	0.804	0.661	1	0.541
Rater3 (3T)	0.767	0.770	0.767	0.761	0.726	0.876	0.702	0.789	0.541	1
CR C5/6	SCT (1.5T)	SCTcor (1.5T)	SCT (3T)	SCTcor (3T)	Rater1 (1.5T)	Rater1 (3T)	Rater2 (1.5T)	Rater2 (3T)	Rater3 (1.5T)	Rater3 (3T)
SCT (1.5T)	1	0.990	0.859	0.859	0.926	0.860	0.853	0.854	0.720	0.858
SCTcor (1.5T)	0.990	1	0.868	0.869	0.922	0.869	0.835	0.850	0.699	0.866
SCT (3T)	0.859	0.868	1	0.999	0.856	0.817	0.797	0.818	0.733	0.859
SCTcor (3T)	0.859	0.869	0.999	1	0.854	0.816	0.792	0.813	0.729	0.858
Rater1 (1.5T)	0.926	0.922	0.856	0.854	1	0.899	0.905	0.853	0.772	0.854
Rater1 (3T)	0.860	0.869	0.817	0.816	0.899	1	0.852	0.873	0.770	0.884
Rater2 (1.5T)	0.853	0.835	0.797	0.792	0.905	0.852	1	0.839	0.868	0.822
Rater2 (3T)	0.854	0.850	0.818	0.813	0.853	0.873	0.839	1	0.732	0.903
Rater3 (1.5T)	0.720	0.699	0.733	0.729	0.772	0.770	0.868	0.732	1	0.719
Rater3 (3T)	0.858	0.866	0.859	0.858	0.854	0.884	0.822	0.903	0.719	1
CSA C5/6	SCT (1.5T)	SCTcor (1.5T)	SCT (3T)	SCTcor (3T)	Rater1 (1.5T)	Rater1 (3T)	Rater2 (1.5T)	Rater2 (3T)	Rater3 (1.5T)	Rater3 (3T)
SCT (1.5T)	1	0.994	0.876	0.876	0.854	0.758	0.880	0.675	0.636	0.682
SCTcor (1.5T)	0.994	1	0.871	0.871	0.834	0.765	0.865	0.672	0.622	0.687
SCT (3T)	0.876	0.871	1	0.999	0.829	0.812	0.765	0.729	0.628	0.700
SCTcor (3T)	0.876	0.871	0.999	1	0.829	0.812	0.762	0.727	0.624	0.696
Rater1 (1.5T)	0.854	0.834	0.829	0.829	1	0.766	0.800	0.784	0.635	0.710
Rater1 (3T)	0.758	0.765	0.812	0.812	0.766	1	0.617	0.776	0.572	0.802
Rater2 (1.5T)	0.880	0.865	0.765	0.762	0.800	0.617	1	0.619	0.666	0.567
Rater2 (3T)	0.675	0.672	0.729	0.727	0.784	0.776	0.619	1	0.669	0.818
Rater3 (1.5T)	0.636	0.622	0.628	0.624	0.635	0.572	0.666	0.669	1	0.603
Rater3 (3T)	0.682	0.687	0.700	0.696	0.710	0.802	0.567	0.818	0.603	1

Table S9 (*continued*)

https://dx.doi.org/10.21037/qims-21-782

Table S9 (*continued*)

CR C6/7	SCT (1.5T)	SCTcor (1.5T)	SCT (3T)	SCTcor (3T)	Rater1 (1.5T)	Rater1 (3T)	Rater2 (1.5T)	Rater2 (3T)	Rater3 (1.5T)	Rater3 (3T)
SCT (1.5T)	1	0.955	0.853	0.823	0.901	0.839	0.805	0.809	0.879	0.798
SCTcor (1.5T)	0.955	1	0.861	0.863	0.881	0.873	0.803	0.834	0.806	0.808
SCT (3T)	0.853	0.861	1	0.982	0.835	0.896	0.795	0.844	0.795	0.858
SCTcor (3T)	0.823	0.863	0.982	1	0.814	0.874	0.785	0.818	0.755	0.808
Rater1 (1.5T)	0.901	0.881	0.835	0.814	1	0.830	0.829	0.810	0.826	0.777
Rater1 (3T)	0.839	0.873	0.896	0.874	0.830	1	0.824	0.905	0.783	0.864
Rater2 (1.5T)	0.805	0.803	0.795	0.785	0.829	0.824	1	0.858	0.801	0.791
Rater2 (3T)	0.809	0.834	0.844	0.818	0.810	0.905	0.858	1	0.808	0.881
Rater3 (1.5T)	0.879	0.806	0.795	0.755	0.826	0.783	0.801	0.808	1	0.725
Rater3 (3T)	0.798	0.808	0.858	0.808	0.777	0.864	0.791	0.881	0.725	1
CSA C6/7	SCT (1.5T)	SCTcor (1.5T)	SCT (3T)	SCTcor (3T)	Rater1 (1.5T)	Rater1 (3T)	Rater2 (1.5T)	Rater2 (3T)	Rater3 (1.5T)	Rater3 (3T)
SCT (1.5T)	1	0.963	0.876	0.874	0.856	0.619	0.870	0.800	0.729	0.723
SCTcor (1.5T)	0.963	1	0.866	0.881	0.790	0.625	0.856	0.793	0.615	0.738
SCT (3T)	0.876	0.866	1	0.989	0.804	0.686	0.753	0.796	0.581	0.743
SCTcor (3T)	0.874	0.881	0.989	1	0.768	0.677	0.748	0.776	0.565	0.719
Rater1 (1.5T)	0.856	0.790	0.804	0.768	1	0.621	0.827	0.742	0.724	0.665
Rater1 (3T)	0.619	0.625	0.686	0.677	0.621	1	0.524	0.660	0.370	0.675
Rater2 (1.5T)	0.870	0.856	0.753	0.748	0.827	0.524	1	0.773	0.751	0.668
Rater2 (3T)	0.800	0.793	0.796	0.776	0.742	0.660	0.773	1	0.572	0.829
Rater3 (1.5T)	0.729	0.615	0.581	0.565	0.724	0.370	0.751	0.572	1	0.446
Rater3 (3T)	0.723	0.738	0.743	0.719	0.665	0.675	0.668	0.829	0.446	1

https://dx.doi.org/10.21037/qims-21-782